

Vector Boson Dark Matter From Trinification

K.S. Babu,^a Sudip Jana,^b Anil Thapa^c

^a*Department of Physics, Oklahoma State University, Stillwater, OK 74078, USA*

^b*Max-Planck-Institut für Kernphysik, Saupfercheckweg 1, 69117 Heidelberg, Germany*

^c*Department of Physics, University of Virginia, Charlottesville, Virginia 22904-4714, USA*

E-mail: babu@okstate.edu, sudip.jana@mpi-hd.mpg.de,
wtd8kz@virginia.edu

ABSTRACT: We show how trinification models based on the gauge group $SU(3)_C \times SU(3)_L \times SU(3)_R$ realized near the TeV scale can provide naturally a variety of dark matter (DM) candidates. These models contain a discrete T parity which may remain unbroken even after spontaneous symmetry breaking. The lightest T -odd particle, which could be a fermion, a scalar, or a gauge boson, can constitute the dark matter of the universe. This framework naturally admits a doublet-singlet fermionic DM, a singlet scalar DM, or a vector boson DM. Here we develop the vector boson DM scenario wherein the DM couples off-diagonally with the usual fermions and vector-like fermions present in the theory. We show consistency of this framework with dark matter relic abundance and direct detection limits as well as LHC constraints. We derive upper limits of 900 GeV on the vector gauge boson DM mass and 4.5 TeV on the vector-like quarks and lepton masses. We also show the consistency of spontaneous gauge symmetry breaking down to Standard Model times an extra $U(1)$ while preserving the T -parity.

KEYWORDS: Dark Matter, Trinification, LHC

Contents

| | | |
|----------|---|-----------|
| 1 | Introduction | 1 |
| 2 | TeV Scale Trinification Model | 4 |
| 2.1 | Fermion mass generation | 5 |
| 2.2 | Gauge boson sector | 6 |
| 2.3 | Higgs potential analysis | 9 |
| 2.3.1 | Necessary conditions for boundedness of the potential | 10 |
| 2.3.2 | Light scalars in the model | 12 |
| 3 | Collider Implications | 13 |
| 4 | Vector Boson Dark Matter Phenomenology | 15 |
| 4.1 | Annihilation cross section and relic abundance | 15 |
| 5 | Conclusion | 19 |
| A | Appendix | 20 |
| A.1 | <i>T</i> -parity even fields | 20 |
| A.1.1 | Weak-triplet scalars | 20 |
| A.1.2 | Weak-doublet scalars | 20 |
| A.1.3 | Weak-singlet scalars | 21 |
| A.2 | <i>T</i> -parity odd fields | 22 |
| A.2.1 | Weak-triplet scalars | 22 |
| A.2.2 | Weak-doublet scalars | 23 |
| A.2.3 | Weak-singlet scalars | 24 |

1 Introduction

Models based on the gauge symmetry $SU(3)_C \times SU(3)_L \times SU(3)_R$, termed trinification [1], were proposed as grand unified theories where matter fields as well as the forces acting on them are unified [1–7]. This is possible owing to the three identical $SU(3)$ factor groups by imposing a cyclic permutation symmetry among them. The three gauge couplings will then all be equal at the scale where the trinification symmetry is realized. This scale turns out to be of order 10^{14} GeV in such a framework as can be inferred by extrapolating the three gauge couplings of the Standard Model (SM) to higher energies.

The trinification gauge structure may be interesting in itself, without necessarily imposing the cyclic permutation symmetry. In this scenario trinification can be realized around the TeV scale, which would make it accessible directly to collider experiments. Many of the

merits of the unified framework would be preserved in this setup, including the quantization of electric charge (since the gauge symmetry is non-Abelian), structure of matter multiplets and inter-relations among fermion masses. These models are asymptotically free and can be extrapolated all the way up to the Planck scale [6], in contrast to the case in the SM. Unlike unified theories based on simple groups such as $SU(5)$, the trinification symmetry group does not have gauge boson mediated proton decay, facilitating its realization near the TeV scale. It is this class of models with TeV scale realization that is the focus of this paper.

The main goal of this paper is to show how a variety of dark matter candidates arises naturally within the trinification framework, and develop the phenomenology of one such scenario where the DM candidate is a vector gauge boson. Natural identification of DM candidates is possible owing to a discrete trinification parity (T -parity) that remains unbroken even after spontaneous symmetry breaking. The T parity is defined as

$$T = (-1)^{I_{8L} + I_{8R} + 2S}, \quad (1.1)$$

where I_{8L} and I_{8R} are the charges (generalized isospins) under the diagonal generators T_{8L} of $SU(3)_L$ and T_{8R} of $SU(3)_R$ and S is the spin of the particle. Previous studies of symmetry breaking in trinification models also broke this T -parity [2–7]. Here we show by explicit construction how to consistently achieve symmetry breaking while preserving T -parity.

The types of DM candidates that can arise within this framework are few and thus predictive. The anomaly-free fermion representations of the theory contain new quarks and leptons which transform chirally under the full symmetry group, but vectorially under the SM gauge symmetry. These new vector-like fermions are T -odd, and the lightest neutral particle among them may be identified as the DM candidate. The quantum numbers of these fermions are fixed by the gauge structure, and thus the nature of such a fermionic DM candidate is fully determined. It turns out this candidate is a mixed doublet-singlet fermion under the weak $SU(2)_L$ symmetry. Unlike the usually discussed doublet-singlet fermion DM models [8–11], here the DM mass is protected by a gauge symmetry. Such a chiral fermion DM is more appealing [12–14]. Since this scenario has been well studied in the literature, here we do not discuss it in any detail, except to note that there would be some differences in its phenomenology owing to couplings of the DM fermion with additional particles (gauge bosons and Higgs bosons) that are present in the theory. In the next section we identify this fermionic DM candidate and briefly comment on the correlation of its mass with the mass of the right-handed neutrino involved in the seesaw mechanism.

The symmetry breaking sector, which we develop in detail here, also has T -odd scalars, the lightest of which may be a dark matter candidate. These particles are either singlets, doublets, or triplets of the weak $SU(2)_L$ gauge group. This restriction arises since we use only two types of Higgs fields for symmetry breaking with quantum numbers $(1, 3, 3^*)$ and $(1, 6, 6^*)$. The first is needed to generate quark and lepton masses, including the vector-like fermion masses, and the second is needed to realize the seesaw mechanism. Thus the DM candidate could be a linear combination of three multiplets – singlet, doublet and triplet – of weak $SU(2)_L$. However, as we show by an explicit Higgs potential analysis, among these scalars, only a T -odd singlet survives down to the TeV scale, if the trinification

symmetry breaks at a higher scale down to the SM times a $U(1)$. There are also two T -even singlet scalars at or below the TeV scale, into which this DM scalar can annihilate. Thus this scenario is very similar to complex singlet DM models where a stable scalar singlet annihilates into its unstable scalar partners [15, 16].

Fermionic or bosonic dark matter candidates which are naturally stable have been studied in the context of the SM with an extended particle spectrum [17], left-right symmetric theories [18], and unified theories based on $SO(10)$ [19, 20]. In these models, typically new fields are introduced to serve the role of DM, with their stability ensured by remnants of the gauge symmetry. In the trinification framework, these new particles are already present with the minimal setup, along the T -parity to stabilize them. This framework can be embedded into E_6 unified theories while preserving the T -parity [21].

Our main focus here is however a T -odd gauge boson dark matter candidate that is available in the theory. It is electrically neutral and also a singlet of the SM gauge symmetry. It has the feature that it couples off-diagonally to fermions and scalars. For example, it connects the T -even SM fermions with the T -odd vector-like fermions, and similarly in the scalar sector. While the trinification symmetry group has several new gauge bosons, the DM candidate we identify originates from the symmetry breaking chain

$$\begin{aligned} SU(3)_C \times SU(3)_L \times SU(3)_R &\rightarrow SU(3)_C \times SU(2)_L \times U(1)_Y \times O(2)_R \\ &\rightarrow SU(3)_C \times SU(2)_L \times U(1)_Y . \end{aligned} \quad (1.2)$$

Here at the first stage of symmetry breaking an $O(2)$ symmetry is left unbroken, along with the SM gauge symmetry. The gauge boson of this $O(2)$ is the dark matter candidate that we analyze in detail. Although the $O(2)$ symmetry is isomorphic with a $U(1)$, we denote it as $O(2)$ in order to emphasize the off-diagonal nature of its couplings to fermions. The first stage of symmetry breaking in Eq. (1.2) is achieved by a Higgs field transforming as $(1, 6, 6^*)$ under the trinification gauge group. This Higgs multiplet also generates Majorana masses for the right-handed neutrinos via renormalizable couplings. The second stage of symmetry breaking is mediated via Higgs fields which transform as $(1, 3, 3^*)$ under trinification. These fields are needed to also break the electroweak symmetry and to provide masses to quarks and leptons. Our analysis shows that this vector boson DM candidate is consistent with relic abundance constraints as well as LHC limits. In fact, we find an upper limit of 900 GeV on its mass, along with upper limits of 4.5 TeV on the vector-like quarks and leptons of the model. The entire parameter space of the model would be probed by future colliders.

Vector boson DM candidates have been studied in several other contexts [22–25]. The trinification DM differs from most of this class in that the gauge interactions of the DM in our framework is completely determined in terms of $SU(2)_L \times U(1)_Y$ gauge couplings. This makes the model more constrained and predictive. The spectrum of particles at or around the TeV scale in the model we analyze consists of the vector boson DM, three families of vector-like quarks and leptons, a new Higgs boson h' which is a remnant of the $O(2)_R$ symmetry breaking, a T -odd scalar singlet H' , and a T -even scalar \tilde{h} as well as a doubly charged T -odd scalar δ^{++} . The last three particles in this list arise as a consequence of symmetry breaking within the minimal setup.

The rest of the paper is organized as follows. In Sec. 2 we describe the trinification model and the symmetry breaking pattern. The gauge boson masses and the Higgs potential are constructed here, with details of the Higgs spectrum delegated to an Appendix. In Sec. 3 we analyze LHC constraints on vector-like leptons and quarks, with their signature decays into leptons/quarks plus missing transverse energy. In Sec. 4 we analyze the dark matter relic abundance and identify parameter space consistent with direct detection and LHC constraints. In Sec. 5 we conclude.

2 TeV Scale Trinification Model

The trinification model is based on the gauge symmetry $SU(3)_C \times SU(3)_L \times SU(3)_R$ under which quarks and leptons fields are assigned as

$$Q_L(3, 3^*, 1) = \begin{pmatrix} u \\ d \\ D \end{pmatrix}_L, \quad Q_R(3, 1, 3^*) = \begin{pmatrix} u \\ d \\ D \end{pmatrix}_R, \quad \psi_L(1, 3, 3^*) = \begin{pmatrix} E^0 & E^- & e^- \\ E^+ & E^{c0} & \nu \\ e^c & \nu^c & N \end{pmatrix}_L. \quad (2.1)$$

Here D_L and D_R are new vector-like iso-singlet quarks under the SM, while (E^0, E^+) and (E^-, E^{c0}) are vector-like lepton doublets with hypercharge $Y = +1/2$ and $-1/2$ respectively. ν^c is the conjugate of the right-handed neutrino, while N is a new neutral singlet of the SM. The $SU(2)_L$ and $SU(2)_R$ subgroups in Eq. (2.1) respectively run vertically and horizontally. Note that e^c and e^- are grouped in the same gauge multiplet which implies that lepton number is explicitly broken in the model.

To break the trinification symmetry spontaneously all the way down to $SU(3)_C \times U(1)_{em}$, we employ three copies of bi-triplet Higgs fields $\Phi_n \sim (1, 3, 3^*)$ and a bi-sextet scalar field $\chi \sim (1, 6, 6^*)$. Three copies of the Φ fields are used so that there are no obvious relations among the fermion masses, which could potentially go wrong. The field content of the Φ_n is analogous to the lepton field in Eq. (2.1). We denote its components as Φ_i^α . The bi-sextet field χ is represented tensorially as $\chi_{ij}^{\alpha\beta}$ and its components can be identified from the coupling $\Phi\Phi\chi^*$ which is gauge invariant. The vacuum expectation values (VEVs) of these Higgs fields are denoted as

$$\langle \Phi_n \rangle = \begin{pmatrix} v_{un} & 0 & 0 \\ 0 & v_{dn} & 0 \\ 0 & 0 & V_n \end{pmatrix}, \quad \langle \chi_{33}^{22} \rangle = V_\nu, \quad \langle \chi_{33}^{33} \rangle = V_N. \quad (2.2)$$

Note that the $\langle \Phi_2^3 \rangle$, the VEV of the ν^c like scalar, see Eq. (2.1), could be nonzero in general, but if it is zero, an unbroken T -parity can be realized. In models with multiple Φ_n fields and no analog of the χ field, trinification symmetry breaking down to the SM would require some $\langle \Phi_2^3 \rangle$ to be nonzero, which would break the T -parity. With only the Φ_n fields acquiring VEVs as in Eq. (2.2), trinification symmetry breaks down to $SU(3)_C \times SU(2)_L \times SU(2)_R \times U(1)$, suggesting the need for an additional scalar field. The bi-sextet field χ serves this role. From the χ field, $\langle \chi_{23}^{33} \rangle$, the VEV of the $(\nu^c N)$ component, could be nonzero in general, but T -parity can be preserved if it is zero. Only the $(\nu^c \nu^c)$ and (NN) components of χ

acquire VEVs, but this is sufficient for reducing the gauge symmetry down to the SM. This is the main difference in our construction compared to other symmetry breaking patterns in trinification [1–6].

We note that the T -parity of a general tensor representation $X_{ijk\dots}^{\alpha\beta\gamma\dots}$ is given by $(-1)^{i+j+k+\dots+\alpha+\beta+\gamma+\dots+2S}$. Under T -parity, all SM fermions are then even, including the ν^c field, while the vector-like fermions $D_L, D_R, (E^0, E^+)$ and (E^-, E^{c0}) are odd. A similar classification can be made for the scalar fields as well.

The VEVs of χV_ν and V_N , can be chosen to be equal and much larger than the VEVs of Φ_n . In this case we can identify the two stage symmetry breaking shown in Eq. (1.2). The identification $V_N = V_\nu$ is supported by the Higgs potential, as we show below. Once the smaller Φ_n VEVs develop, the equality $V_N = V_\nu$ can no longer be preserved, owing to an induced value of $V_N - V_\nu$ which could be of order V_n , the smaller VEV. This is the scenario that we investigate which yields a TeV scale vector boson dark matter candidate, with all other gauge bosons being heavier than a few TeV.

2.1 Fermion mass generation

There are 27 Weyl fermions per generation of $\{Q_L \oplus Q_R \oplus \psi_L\}$ of which 15 are the usual SM chiral fermions, the ν^c field is the singlet fermion involved in the seesaw mechanism, and the remaining 10 fields are vector-like iso-singlet quarks and iso-doublet leptons. As noted earlier, in order to generate the observed pattern of quark and lepton masses, three copies of $\Phi_n \sim (1, 3, 3^*)$ Higgs fields and one $\chi \sim (1, 6, 6^*)$ field are introduced. The most general Yukawa interactions of quark and leptons with these Higgs fields are given by

$$-\mathcal{L}_Y = Y_{qn} \bar{Q}_{L\alpha} (\Phi_n)_i^\alpha Q_{Ri} + Y_{\ell n} \psi_i^\alpha \psi_j^\beta (\Phi_n)_k^\gamma \epsilon^{ijk} \epsilon_{\alpha\beta\gamma} + y_\ell \psi_i^\alpha \psi_j^\beta \chi_{\alpha\beta}^{ij} + h.c., \quad (2.3)$$

where $(i, j, k, \alpha, \beta, \gamma)$ are $SU(3)$ indices, and $Y_{qn}, Y_{\ell n}$, and y_ℓ are 3×3 Yukawa coupling matrices, with y_ℓ being symmetric. We have suppressed generation indices here. Expanding in component form the mass matrices for up-type, down-type and vector-like quarks are found as

$$M_u = Y_{qn} v_{un}, \quad M_d = Y_{qn} v_{dn}, \quad M_D = Y_{qn} V_n. \quad (2.4)$$

This shows the need for multiple copies of Φ_n fields. With a single Φ field all three matrices would become proportional, resulting in no quark mixing. Even with two copies of Φ , the vector-like quark mass matrix can be derived from those of the light quarks, which does not support TeV scale realization of trinification [7]. With three copies of Φ_n , all fermion masses and mixings can be accommodated, along with TeV scale symmetry breaking.

The mass matrices for the charged lepton read as

$$M_e = -Y_{\ell n} v_{dn}, \quad M_{E^\pm} = -Y_{\ell n} V_n. \quad (2.5)$$

This three copies of Φ_n would give the flexibility to give independent masses to the leptons and the vector-like leptons as well. In the neutral lepton sector the mass matrices decouple into a $2N_g \times 2N_g$ matrix and a $3N_g \times 3N_g$ matrix where N_g is the number of generation,

which read as

$$M_\nu = \begin{pmatrix} 0 & -Y_{\ell n} v_{un} \\ -Y_{\ell n} v_{un} & y_\ell V_\nu \end{pmatrix}, \quad M_N = \begin{pmatrix} 0 & Y_{\ell n} V_n & Y_{\ell n} v_{un} \\ Y_{\ell n} V_n & 0 & Y_{\ell n} v_{dn} \\ Y_{\ell n} v_{un} & Y_{\ell n} v_{dn} & y_\ell V_N \end{pmatrix}. \quad (2.6)$$

Here M_ν spans the basis (ν, ν^c) and M_N spans the basis (E^{c0}, E^0, N) . Note that in the electroweak symmetric limit, obtained by setting v_{un} and v_{dn} to zero, the field N decouples, while the mass of vector-like neutral doublet and E^\pm become degenerate, as they form an $SU(2)$ doublet. The light neutrino mass matrix can be obtained from the 6×6 matrix M_ν of Eq. (2.6). In the limit of $Y_{\ell n} v_{un} \ll y_\ell V_\nu$, the 3×3 light neutrino mass matrix can be obtained from usual seesaw mechanism as

$$m_\nu^{\text{light}} \simeq -(Y_{\ell n} v_{un})(y_\ell V_\nu)^{-1}(Y_{\ell n} v_{un}). \quad (2.7)$$

The mass matrix for the heavier state is simply $y_\ell V_\nu$.

The decoupling of the matrices in Eq. (2.6) is due to T -parity under which ν and ν^c are even, while (E^{c0}, E^0, N) are odd. The lightest of these T -odd states can be a dark matter candidate. This is the singlet-doublet DM scenario studied extensively [8–11]. As already noted, one difference here is the chiral nature of the DM fermion under the full symmetry which protects its mass. Stability of the DM is guaranteed by a discrete gauge symmetry, the T -parity of the model. Furthermore, the singlet-doublet DM mass matrix is closely related to the neutrino mass matrix as seen from Eq. (2.6). Note in particular that the Majorana mass matrices of the ν^c and N fields are proportional. Since we are interested in the case where $V_N \simeq V_\nu \gg V_n$, from the T -odd neutral lepton mass matrix it is possible to integrate out the N field, which would provide a small Majorana mass correction to the nearly degenerate Dirac fermion doublet. Since this Majorana mass should be of at least of order 100 keV to be consistent with DM direct detection, we see that V_N cannot be many orders of magnitude larger than V_n .

2.2 Gauge boson sector

In this section, we examine the gauge boson sector and obtain all the mass eigenvalues and eigenstates explicitly. In particular, we find that one of the 12 new gauge bosons can be lighter than the rest and be a potential DM candidate.

At the scale of $SU(3)_L \times SU(3)_R$ unification the gauge couplings are related as

$$\alpha_R^{-1} = \frac{3}{4}\alpha_Y^{-1} - \frac{1}{4}\alpha_L^{-1}. \quad (2.8)$$

The gauge couplings α_L and α_R at a given energy scale can be calculated from the measured values of the low energy gauge couplings at $\mu = m_Z$. We take as input $\alpha_{em}(m_Z) = 1/127.940$ and $\sin^2 \theta_W(m_Z) = 0.23126$, which give $\alpha_L(m_Z) = 0.033798$ and $\alpha_Y(m_Z) = 0.010675$ for the $SU(2)_L$ and $U(1)_Y$ fine structure constants. Here $\alpha_{em}^{-1} = \alpha_L^{-1} + \alpha_Y^{-1}$ is used to obtain the value of α_Y . We then use one-loop renormalization group equations to evaluate α_i to higher energy scales, with the beta function coefficients given by $b_i = 41/6$ ($-19/6$)

for $\alpha_{L(Y)}$ with contributions arising only from the SM particles. With these, we find that the ratio of $\alpha_R/\alpha_L = 0.49$ at around TeV scale.

The field Φ_n transforms as $\Phi_n \rightarrow U_L \Phi_n U_R^\dagger$ under gauge symmetry. The transformation of the χ field can be obtained from here in tensorial form. The covariant derivatives for the Higgs fields can then be written as

$$\mathcal{L}_{gauge} = \sum_n D^\mu(\Phi_n)_i^\alpha D_\mu(\Phi_n)_\alpha^i + \sum_{\alpha\beta ij} (D_\mu \chi_{ij}^{\alpha\beta}) (D^\mu \chi_{\alpha\beta}^{ij}), \quad (2.9)$$

where

$$D^\mu(\Phi_n)_i^\alpha = \partial^\mu(\Phi_n)_i^\alpha - \frac{ig_L}{2} (\vec{T} \cdot \vec{W}_L^\mu)_i^k (\Phi_n)_k^\alpha + \frac{ig_R}{2} (\vec{T} \cdot \vec{W}_R^\mu)_k^\alpha (\Phi_n)_i^k, \quad (2.10)$$

$$\begin{aligned} D^\mu \chi_{ij}^{\alpha\beta} &= \partial^\mu \chi_{ij}^{\alpha\beta} - \frac{ig_L}{2} (\vec{T} \cdot \vec{W}_L^\mu)_i^k \chi_{kj}^{\alpha\beta} - \frac{ig_L}{2} (\vec{T} \cdot \vec{W}_L^\mu)_j^k \chi_{ik}^{\alpha\beta} \\ &\quad + \frac{ig_R}{2} (\vec{T} \cdot \vec{W}_R^\mu)_\gamma^\alpha \chi_{ij}^{\gamma\beta} + \frac{ig_R}{2} (\vec{T} \cdot \vec{W}_R^\mu)_\gamma^\beta \chi_{ij}^{\alpha\gamma}. \end{aligned} \quad (2.11)$$

We define the gauge boson multiplets in the $(1, 8, 1)_L$ and $(1, 1, 8)_R$ representation as

$$\vec{T} \cdot \vec{W}_{L,R}^\mu = \begin{pmatrix} W_3 + \frac{W_8}{\sqrt{3}} & \sqrt{2}W^+ & \sqrt{2}V^+ \\ \sqrt{2}W^- & -W_3 + \frac{W_8}{\sqrt{3}} & \sqrt{2}V^0 \\ \sqrt{2}V^- & \sqrt{2}V^{0*} & \frac{-2W_8}{\sqrt{3}} \end{pmatrix}^\mu_{L,R}, \quad (2.12)$$

with the following definitions:

$$W^{\pm\mu} = \frac{W_1^\mu \mp iW_2^\mu}{\sqrt{2}}, \quad V^{\pm\mu} = \frac{W_4^\mu \mp iW_5^\mu}{\sqrt{2}}, \quad V^{0(*)\mu} = \frac{W_6^\mu \mp iW_7^\mu}{\sqrt{2}}. \quad (2.13)$$

Here $(V^{\mu+}, V^{\mu 0})_{L,R}$ form $SU(2)_{L,R}$ doublets, while $(W_8^\mu)_{L,R}$ are singlets. Note that with the choice of our VEV structure which leads to T -parity conservation, there is no mixing between $W^{\mu\pm}$ and $V^{\mu\pm}$ fields which are even and odd respectively under T .

The T -even charged gauge boson mass matrix reads, in the basis $(W_L^{\mu+}, W_R^{\mu+})$, as

$$M_{W_{L,R}^+}^2 = \frac{1}{2} \begin{pmatrix} g_L^2(v_{dn}^2 + v_{un}^2) & -2g_L g_R v_{dn} v_{un} \\ -2g_L g_R v_{dn} v_{un} & g_R^2(v_{dn}^2 + v_{un}^2 + 2V_\nu^2) \end{pmatrix}. \quad (2.14)$$

The mixing angle between W_L^\pm and W_R^\pm is strongly constrained to be $\leq 4 \times 10^{-3}$ from strangeness changing nonleptonic decays of hadrons [26], as well as from $b \rightarrow s\gamma$ decay [27], independent of the mass of the heavier W_R^\pm state. LHC experiments have set a lower limit of about 4 TeV on W_R^\pm mass from its production and subsequent decays into dijets, which translates into a lower limit of $V_\nu > 9$ TeV within the model.

The remaining T -odd charged gauge bosons mass matrix is given in the basis $(V_L^{\mu+}, V_R^{\mu+})$ as

$$M_{V_{L,R}^+}^2 = \frac{1}{2} \begin{pmatrix} g_L^2(v_{un}^2 + V_n^2 + 2(V_N^2 + V_\nu^2)) & -2g_L g_R v_{un} V_n \\ -2g_L g_R v_{un} V_n & g_R^2(v_{un}^2 + V_n^2 + 2V_N^2) \end{pmatrix}. \quad (2.15)$$

In the neutral gauge boson sector, the T -odd $V_{L,R}^{\mu 0}$ fields decouple from rest of the gauge bosons, with no mixing among its real and imaginary components defined in Eq. (2.13). The mass matrix for the real components in the basis (W_{6L}^μ, W_{6R}^μ) reads as

$$M_{W_{6LR}}^2 = \frac{1}{2} \begin{pmatrix} g_L^2(v_{dn}^2 + V_n^2 + 2(V_N^2 + V_\nu^2)) & -2g_L g_R v_{dn} V_n \\ -2g_L g_R v_{dn} V_n & g_R^2(v_{dn}^2 + V_n^2 + 2(V_N + V_\nu)^2) \end{pmatrix}. \quad (2.16)$$

The mass matrix for the imaginary components in the basis (W_{7L}^μ, W_{7R}^μ) reads as

$$M_{W_{7LR}}^2 = \frac{1}{2} \begin{pmatrix} g_L^2(v_{dn}^2 + V_n^2 + 2(V_N^2 + V_\nu^2)) & -2g_L g_R v_{dn} V_n \\ -2g_L g_R v_{dn} V_n & g_R^2(v_{dn}^2 + V_n^2 + 2(V_N - V_\nu)^2) \end{pmatrix}. \quad (2.17)$$

As can be seen from these equations, one of the eigenstates can be relatively light in the limit $V_N \simeq V_\nu \gg V_n$. We define a parameter a as

$$(V_N - V_\nu) = a V_n \quad (2.18)$$

which we shall see is consistent with the minimization of the Higgs potential (cf. Eq. (A.60) in Appendix). With this hierarchy of VEVs, W_{7R} is lighter than all the other states, which we identify as the vector boson dark matter candidate. Choosing $V_N = 9$ TeV, which is the lowest allowed value in this scheme from W_R mass limits, the masses of $(W_R^{\mu+}, V_L^{\mu+}, V_R^{\mu+}, W_{6L}^\mu, W_{6R}^\mu, W_{7L}^\mu)$ are respectively (3.96, 8.0, 3.96, 8.0, 7.92, 8.0) TeV.

In the T -even neutral gauge boson sector there is mixing among $(W_{3L}^\mu, W_{3R}^\mu, W_{8L}^\mu, W_{8R}^\mu)$ to produce the physical A^μ , Z_L^μ , Z_{1R}^μ , and Z_{2R}^μ states, We adopt the following convenient field definitions:

$$A^\mu = \frac{\sqrt{3}g_R W_{3L}^\mu + \sqrt{3}g_L W_{3R}^\mu + g_R W_{8L}^\mu + g_L W_{8R}^\mu}{2\sqrt{g_L^2 + g_R^2}}, \quad (2.19)$$

$$Z_L^\mu = \frac{(g_R^2 + 4g_L^2) W_{3L}^\mu - 3g_L g_R W_{3R}^\mu - \sqrt{3}g_R^2 W_{8L}^\mu - \sqrt{3}g_L g_R W_{8R}^\mu}{2\sqrt{(g_L^2 + g_R^2)(4g_L^2 + g_R^2)}}, \quad (2.20)$$

$$Z_{1R}^\mu = \frac{-g_L W_{8L}^\mu + g_R W_{8R}^\mu}{\sqrt{g_L^2 + g_R^2}}, \quad (2.21)$$

$$Z_{2R}^\mu = \frac{-(g_L^2 + g_R^2) W_{3R}^\mu + \sqrt{3}g_L g_R W_{8L}^\mu + \sqrt{3}g_L^2 W_{8R}^\mu}{\sqrt{(g_L^2 + g_R^2)(4g_L^2 + g_R^2)}}. \quad (2.22)$$

In this basis, the photon field decouples from the rest, reducing the mass matrix to a 3×3 matrix defined as

$$(M_{Z_{LR}}^2)_{ij} = m_{ij}, \quad (2.23)$$

where m_{ij} read as

$$m_{11} = \frac{2g_L^2(g_L^2 + g_R^2)(v_{dn}^2 + v_{un}^2)}{4g_L^2 + g_R^2}, \quad (2.24)$$

$$m_{12} = \frac{g_L(g_L^2 + g_R^2)(v_{dn}^2 - v_{un}^2)}{\sqrt{3}(4g_L^2 + g_R^2)}, \quad (2.25)$$

$$m_{13} = \frac{g_L g_R (g_L^2 + g_R^2)(v_{dn}^2 + v_{un}^2)}{4g_L^2 + g_R^2} \quad (2.26)$$

$$m_{22} = \frac{1}{6(g_L^2 + g_R^2)} [(g_L^2 + g_R^2)^2 (v_{dn}^2 + v_{un}^2 + 4(4V_N^2 + V_n^2)) + 4(g_R^2 - 2g_L^2)V_\nu^2], \quad (2.27)$$

$$m_{23} = \frac{g_R(g_L^2 + g_R^2)^2 (v_{dn}^2 - v_{un}^2) + 4g_R(-8g_L^4 + 2g_L^2 g_R^2 + g_R^4)V_\nu^2}{2\sqrt{3}(g_L^2 + g_R^2)\sqrt{4g_L^2 + g_R^2}}, \quad (2.28)$$

$$m_{33} = \frac{g_R^2(g_L^2 + g_R^2)(v_{dn}^2 + v_{un}^2)}{2(4g_L^2 + g_R^2)} + \frac{2g_R^2(4g_L^2 + g_R^2)V_\nu^2}{g_L^2 + g_R^2}. \quad (2.29)$$

In the limit of unbroken electroweak symmetry, the masses for the heavy neutral fields are given by

$$M_{Z'_1, Z'_2}^2 = \frac{1}{3} \left((g_L^2 + g_R^2)(V_n^2 + 4(V_N^2 + V_\nu^2)) \mp \sqrt{\Delta} \right), \quad (2.30)$$

where $\Delta = (g_L^2 + g_R^2)^2 [(4V_N^2 + V_n^2)^2 + 16V_\nu^4] + 4(2g_L^2 - 8g_L^2 g_R^2 - g_R^4)(4V_N^2 + V_n^2)V_\nu^2$. In the limit where $V_N - V_\nu \ll V_N$ as defined in Eq. (2.18) and to the zeroth order in V_n we have

$$M_{Z'_1, Z'_2}^2 = \frac{4}{3} V_N^2 [2(g_L^2 + g_R^2) \mp | -2g_L^2 + g_R^2 |]. \quad (2.31)$$

If we set here the experimental lower limit of about 5 TeV on the Z' mass from LHC searches, we would find $V_N \geq 5.7$ TeV, which is less stringent than the 9 TeV limit obtained from the W_R searches at the LHC. The masses of the gauge bosons (Z'_1, Z'_2) when $V_N = 9$ TeV are found to be (7.92, 13.8) TeV.

2.3 Higgs potential analysis

Here we construct and analyze the Higgs potential involving one copy of $(1, 3, 3^*)$, denoted by Φ_i^α with i and α being the $SU(3)_L$ and $SU(3)_R$ indices and one copy of $(1, 6, 6^*)$ field, denoted as $\chi_{ij}^{\alpha\beta}$. The field χ obeys the symmetry properties $\chi_{ij}^{\alpha\beta} = \chi_{ji}^{\alpha\beta} = \chi_{ij}^{\beta\alpha}$. While the full theory contains two additional copies of $\Phi(1, 3, 3^*)$ fields, here we note that only one combination of the three, defined as $(V_1\Phi_1 + V_2\Phi_2 + V_3\Phi_3)/\sqrt{V_1^2 + V_2^2 + V_3^2}$, acquires a VEV along the SM singlet direction, while the two orthogonal combinations to this state only acquire electroweak scale VEVs. It is this field with the VEV along the SM singlet direction that we keep in our analysis, which we denote simply as Φ_i^α . This should be an excellent approximation, as we ignore electroweak symmetry breaking effects in our analysis. Certain scalar fields will be found to have masses below $V_N \simeq V_\nu$, which would be also maintained even with the inclusion of two additional Φ fields. The terms involving these additional Φ fields can mix the fields we keep, which would only lower the masses of the unmixed states further.

The most general renormalizable potential for (χ, Φ) can be written as

$$V = V(\chi) + V(\phi) + V(\Phi, \chi), \quad (2.32)$$

where

$$\begin{aligned}
V(\chi) = & -m_\chi^2 \chi_{ij}^{\alpha\beta} \chi_{\alpha\beta}^{ij} + \{\mu_\chi \chi_{ij}^{\alpha\beta} \chi_{kl}^{\gamma\delta} \chi_{mn}^{\mu\nu} \epsilon^{ikm} \epsilon^{jln} \epsilon_{\alpha\gamma\mu} \epsilon_{\beta\delta\nu} + h.c.\} \\
& + \lambda_1 \chi_{ij}^{\alpha\beta} \chi_{\alpha\beta}^{ij} \chi_{kl}^{\gamma\delta} \chi_{\gamma\delta}^{kl} + \lambda_2 \chi_{ij}^{\alpha\beta} \chi_{\alpha\gamma}^{ij} \chi_{kl}^{\gamma\delta} \chi_{\beta\delta}^{kl} + \lambda_3 \chi_{ij}^{\alpha\beta} \chi_{\gamma\delta}^{ij} \chi_{kl}^{\gamma\delta} \chi_{\alpha\beta}^{kl} \\
& + \lambda_4 \chi_{ij}^{\alpha\beta} \chi_{\alpha\beta}^{jk} \chi_{kl}^{\gamma\delta} \chi_{\gamma\delta}^{li} + \lambda_5 \chi_{ij}^{\alpha\beta} \chi_{\alpha\gamma}^{jk} \chi_{kl}^{\gamma\delta} \chi_{\beta\delta}^{li} .
\end{aligned} \tag{2.33}$$

Here we have used the notation $\chi_{\alpha\beta}^{ij} = (\chi_{ij}^{\alpha\beta})^*$. By a field redefinition, μ_χ can be made real, in which case the vacuum admits a solution where the VEVs from χ are also real. The remaining parts of the potential are given by

$$V(\Phi) = -m_\Phi^2 \Phi_i^\alpha \Phi_\alpha^i + \{\mu_\Phi \Phi_i^\alpha \Phi_j^\beta \Phi_k^\gamma \epsilon^{ijk} \epsilon_{\alpha\beta\gamma} + h.c.\} + \lambda_6 \Phi_i^\alpha \Phi_\alpha^i \Phi_j^\beta \Phi_\beta^j + \lambda_7 \Phi_i^\alpha \Phi_\alpha^j \Phi_j^\beta \Phi_\beta^i , \tag{2.34}$$

and

$$\begin{aligned}
V(\Phi, \chi) = & \{\mu_{\phi\chi} \Phi_i^\alpha \Phi_j^\beta \chi_{\alpha\beta}^{ij} + h.c.\} + \lambda_8 \Phi_i^\alpha \Phi_\alpha^i \chi_{jk}^{\beta\gamma} \chi_{\beta\gamma}^{jk} + \lambda_9 \Phi_i^\alpha \Phi_\beta^i \chi_{kl}^{\beta\gamma} \chi_{\alpha\gamma}^{kl} \\
& + \lambda_{10} \Phi_i^\alpha \Phi_\alpha^j \chi_{jl}^{\beta\gamma} \chi_{\beta\gamma}^{il} + \lambda_{11} \Phi_i^\alpha \Phi_\beta^j \chi_{jl}^{\beta\gamma} \chi_{\alpha\gamma}^{il} + \left\{ \lambda_{12} \Phi_i^\alpha \chi_{\beta\gamma}^{jk} \chi_{lj}^{\beta\delta} \chi_{mk}^{\kappa\gamma} \epsilon^{ilm} \epsilon_{\alpha\delta\kappa} \right. \\
& \left. + \lambda_{13} \Phi_i^\alpha \Phi_j^\beta \Phi_\gamma^k \chi_{kl}^{\delta\gamma} \epsilon^{ijl} \epsilon_{\alpha\beta\delta} + \lambda_{14} \Phi_i^\alpha \Phi_j^\beta \chi_{kl}^{\gamma\delta} \chi_{mn}^{\rho\sigma} \epsilon^{ikm} \epsilon^{jln} \epsilon_{\alpha\gamma\rho} \epsilon_{\beta\delta\sigma} + h.c. \right\} .
\end{aligned} \tag{2.35}$$

By inserting the VEV of Eq. (2.2) in Eq. (2.32), and using the minimization conditions, mass matrices for the charged and neutral Higgs bosons can be constructed. A complete analysis of the spectrum that includes electroweak symmetry breaking effects is beyond the scope of the present work. However, in the electroweak symmetric limit, the charged, scalar, and pseudoscalar mass matrices in the T -even and T -odd sectors of the theory can be built from the Higgs potential of Eq. (2.32) by setting v_{un} and v_{dn} to zero. We show the consistency of symmetry breaking and identify the light scalars that survive to scales below $V_N \simeq V_\nu$.

By inserting the VEV $\langle \Phi_3^3 \rangle = V_n$, $\langle \chi_{33}^{22} \rangle = V_\nu$, and $\langle \chi_{33}^{33} \rangle = V_N$, we obtain the following condition for the potential to be extremum around the VEVs:

$$\mu_{\phi\chi} V_n^2 + V_N [-m_\chi^2 + 2\lambda V_N^2 + \lambda' V_n^2 + 2(\lambda_1 + \lambda_3 + \lambda_4) V_\nu^2] = 0 , \tag{2.36}$$

$$V_\nu [-m_\chi^2 + (\lambda_{10} + \lambda_8) V_n^2 + 2(\lambda_1 + \lambda_3 + \lambda_4) V_N^2 + 2\lambda V_\nu^2] = 0 , \tag{2.37}$$

$$V_n [-m_\Phi^2 + 2\mu_{\phi\chi} V_N + \lambda' V_N^2 + (\lambda_{10} + \lambda_8) V_\nu^2 + 2(\lambda_6 + \lambda_7) V_n^2] = 0 , \tag{2.38}$$

where we have defined $\lambda = \lambda_1 + \lambda_2 + \lambda_3 + \lambda_4 + \lambda_5$ and $\lambda' = \lambda_8 + \lambda_9 + \lambda_{10} + \lambda_{11}$. We eliminate m_χ^2 , m_Φ^2 , and $\mu_{\phi\chi}$ using these three conditions and keep the VEVs V_N , V_ν and V_n as independent parameters. The full spectrum for the masses of the Higgs fields are given in detail in Appendix A, where SM quantum number each component has been properly identified. We have also identified the 12 Goldstone modes associated with spontaneous breaking of $SU(3)_L \times SU(3)_R$ down to SM gauge symmetry.

2.3.1 Necessary conditions for boundedness of the potential

The full set of necessary and sufficient conditions on the quartic couplings of the potential to be bounded from below is not easily tractable in the model. However, certain necessary

| Parameter | λ_1 | λ_2 | λ_3 | λ_4 | λ_5 | λ_6 | λ_7 | λ_8 | λ_9 | λ_{10} | λ_{11} |
|-----------|----------------|----------------|----------------|-------------|-------------|-------------|-------------|-------------|-------------|----------------|-------------------|
| BP-I | 2.42 | -0.0061 | -0.49 | -1.7 | -0.0053 | 1.77 | 1.68 | 1.87 | 1.89 | -1.71 | 1.76 |
| | λ_{12} | λ_{13} | λ_{14} | a | μ_χ | μ_Φ | V_N | M_{DM} | $M_{h'}$ | $M_{H'}$ | $M_{\delta^{++}}$ |
| | -1.21 | -0.64 | -1.06 | 0.68 | 0.18 | -0.74 | -0.16 | 0.076 | 0.057 | 0.165 | 0.133 |

| Parameter | λ_1 | λ_2 | λ_3 | λ_4 | λ_5 | λ_6 | λ_7 | λ_8 | λ_9 | λ_{10} | λ_{11} |
|-----------|----------------|----------------|----------------|-------------|-------------|-------------|-------------|-------------|-------------|----------------|-------------------|
| BP-II | 1.96 | -0.0061 | -0.18 | -1.42 | -0.0025 | 0.54 | 0.74 | 1.10 | 1.89 | -1.14 | 1.81 |
| | λ_{12} | λ_{13} | λ_{14} | a | V_n | μ_χ | μ_Φ | M_{DM} | $M_{h'}$ | $M_{H'}$ | $M_{\delta^{++}}$ |
| | -1.19 | -0.72 | -1.03 | 0.61 | 0.17 | -0.32 | -0.41 | 0.069 | 0.095 | 0.187 | 0.118 |

Table I: Values of the parameters that satisfies the necessary boundedness conditions defined in Eqs. (2.42)-(2.46) and positivity of the square of mass matrices given in Appendix A. Here all the mass parameter are normalized by trification breaking scale V_N . Masses of all the remaining scalar fields are heavier than $M_{H'}$ and their numerical values are given in Appendix A, with $M_{\tilde{h}} = 0.65$ (0.39) for the BP-I (BP-II).

conditions of phenomenological interest can be analyzed analytically. We focus only on the neutral singlet fields Φ_3^3 , χ_{33}^{22} , and χ_{33}^{33} . The quartic terms $V^{(4)}(\Phi, \chi)$ form a vector space spanned by the real-valued vectors $x^T = \{V_n, V_N, V_\nu\}$ which can be written as

$$V^{(4)} = \frac{1}{2} x^T \hat{\lambda} x, \quad (2.39)$$

where

$$\hat{\lambda} = \begin{pmatrix} \lambda_6 + \lambda_7 & \lambda'/2 & (\lambda_{10} + \lambda_8)/2 \\ \lambda'/2 & \lambda & (\lambda_1 + \lambda_3 + \lambda_4) \\ (\lambda_{10} + \lambda_8)/2 & (\lambda_1 + \lambda_3 + \lambda_4) & \lambda \end{pmatrix} \quad (2.40)$$

is a real symmetric matrix, where $\lambda = \lambda_1 + \lambda_2 + \lambda_3 + \lambda_4 + \lambda_5$ and $\lambda' = \lambda_9 + \lambda_9 + \lambda_{10} + \lambda_{11}$. The necessary and sufficient conditions for the boundedness of this restricted potential can be derived from the co-positivity of the real symmetric matrix $\hat{\lambda}$ of Eq. (2.40), which are [28, 29]:

$$\lambda_6 + \lambda_7 \geq 0, \quad (2.41)$$

$$\lambda \geq 0, \quad (2.42)$$

$$\lambda'/2 \geq -\sqrt{(\lambda_6 + \lambda_7)\lambda}, \quad (2.43)$$

$$(\lambda_{10} + \lambda_8)/2 \geq -\sqrt{(\lambda_6 + \lambda_7)\lambda}, \quad (2.44)$$

$$(\lambda_1 + \lambda_3 + \lambda_4) \geq -\lambda, \quad (2.45)$$

$$\begin{aligned} & \lambda'/2\sqrt{\lambda} + (\lambda_1 + \lambda_3 + \lambda_4)\sqrt{\lambda_6 + \lambda_7} \\ & + 1/2(\lambda_8 + \lambda_{10})\sqrt{\lambda} + \sqrt{(\lambda_6 + \lambda_7)\lambda^2} \geq 0 \text{ or } \det \hat{\lambda} \geq 0. \end{aligned} \quad (2.46)$$

In Table I, we show two benchmark points of the parameter space that satisfies all the necessary boundedness conditions defined in Eqs. (2.42)-(2.46). The same parameter also satisfies the positivity criteria of the mass eigenvalues of all scalar fields given in Appendix A. We have also shown the masses of the lighter states in the theory in Table I. All states

not shown in the table have masses much larger, and we show their numerical values for the two benchmark points in Appendix A.

2.3.2 Light scalars in the model

In this subsection we discuss the light scalar fields that are present in the model in addition to the vector boson DM. The light Higgs states in the model are found to be

$$\{\delta^{++}, h', H', \tilde{h}\} \quad (2.47)$$

which have masses of order V_n , the lower scale of $O(2)_R$ symmetry breaking. Here the h' field can be identified as the remnant of this $O(2)_R$ breaking, while the others remain light owing to the constraints arising from the Higgs potential. H' here is a T -odd field, which makes it a possible candidate for DM in the theory. The other fields in Eq. (2.47) are all T -even scalars.

As can be seen from Eq. (A.16), positivity of the squared mass of δ^{++} demands $\lambda_2 + \lambda_5 < 0$. Furthermore, the positivity condition of the squared mass of the state given in Eq. (A.56) along with the condition of Eq. (2.18) implies that $\lambda_2 + \lambda_5 = b (\lambda_9 + \lambda_{11}) V_n^2/V_N^2$, where b can be order one entry. Thus, the mass of the weak $SU(2)_L$ singlet scalar field given in Eq. (A.56) read as

$$M_{\delta^{++}} = \sqrt{(\lambda_9 + \lambda_{11}) b} V_n. \quad (2.48)$$

Similarly, the mass of T -odd weak-singlet neutral scalar field given in Eq. (A.56) read as

$$M_{H'} = \frac{1}{\sqrt{2}} \sqrt{(1 + 2a^2) (1 + 8b) (\lambda_{11} + \lambda_9)} V_n. \quad (2.49)$$

Note that this field, if lightest T -odd in the model, can be a dark matter candidate which we shall discuss in later section. There are two more T -even weak-singlet neutral scalar fields that can be light, which are linear combination of the fields ($\text{Re}[\chi_{33}^{22}], \text{Re}[\chi_{33}^{33}], \text{Re}[\Phi_3^3]$), and the mass-squared terms are given in Eqs. (A.18)-(A.22). We work in the limit of $V_n/V_N \ll 1$ and make a 45° rotation among the first two states to decouple the heavy state. The resulting mass matrix reads as

$$M^2 = \begin{pmatrix} 8\hat{\lambda} V_\nu (V_\nu + aV_n) & 0 & 0 \\ 0 & \frac{1}{2}(1 + 8b)\tilde{\lambda} V_n^2 & -4\sqrt{2} ab \tilde{\lambda} V_n^2 \\ 0 & -4\sqrt{2} ab \tilde{\lambda} V_n^2 & \left[4(\lambda_6 + \lambda_7) - \frac{(\lambda_{10} + \lambda_8)^2}{\hat{\lambda}}\right] V_n^2 \end{pmatrix}, \quad (2.50)$$

where $\tilde{\lambda} = \lambda_{11} + \lambda_9$ and $\hat{\lambda} = \lambda_1 + \lambda_3 + \lambda_4$. It is clear from the Eq. (2.50) that two of the states have masses proportional to V_n which will remain light. In our numerical study of DM annihilation, for concreteness we work in the limit of $ab \ll 1$ so that these two light states become pure states. We denote the second state as \tilde{h} and the third state as h' . Note that if h' and \tilde{h} are lighter than DM, gauge boson DM can annihilate into pairs of these states.

We briefly comment on the possibility of scalar DM within the theory. The state H' is a SM singlet and T -odd. If it is the lightest T -odd particle, it would constitute the DM of

the universe. Unlike the scalar singlet DM model within the context of SM [30, 31], here H' can annihilate into pairs of h' and \tilde{h} , provided that these T -even scalars are lighter than H' . There would be a significant region of allowed parameter space, analogous to complex singlet DM [15, 16].

3 Collider Implications

This model allows for the testing of TeV scale trinification at the Large Hadron Collider (LHC). The existence of vector-like quarks and vector-like leptons, in addition to vector boson dark matter, results in a rich phenomenology for the LHC. In this section, we explore the potential smoking gun signals associated with vector boson dark matter and current LHC constraints.

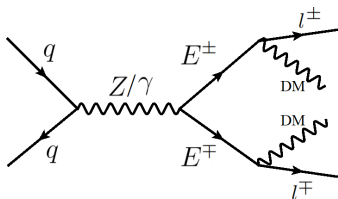


Figure 1: Representative Feynman diagrams for vector like lepton productions and subsequent decays at the LHC.

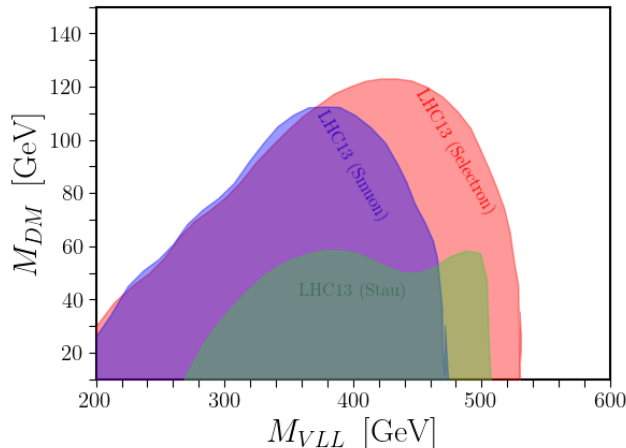


Figure 2: Current LHC limits on vector like leptons in our model.

Vector-like leptons will be dominantly pair-produced at the LHC through the s -channel Z/γ exchange (see Fig. 1), and then decay to leptons and vector boson dark matter, yielding a promising $pp \rightarrow l^+l^- + \cancel{E}_T$ signature. This will resemble the signals of supersymmetric slepton searches [32, 33] leading to dilepton and missing energy signatures. It is worth noting that the pair-production rate of vector-like leptons (fermion) in our scenario is substantially larger than the pair-production rate of slepton (scalar). Non-observation

of any new physics signal in the $pp \rightarrow l^+l^- + \cancel{E}_T$ channel [32, 33], on the other hand, imposes tight bounds on the sub-TeV vector-like lepton masses. We recast the bounds on the vector-like leptons in our model using the most current selectron [33], smuon [33], and stau [32] search limits. In order to do that, we implement our model file in the `FeynRules` package [34] and then compute the signal cross sections using `MadGraph5aMC@NLO` [35]. Then, assuming that the cut efficiencies are identical in both scenarios, we compare the signal cross-sections to the experimental upper bounds. We find that the selectron search [33] yields the most stringent constraint on the vector-like lepton mass, with the exclusion region reaching ~ 630 GeV. We summarize these current LHC limits on the vector-like leptons in Fig. 2.

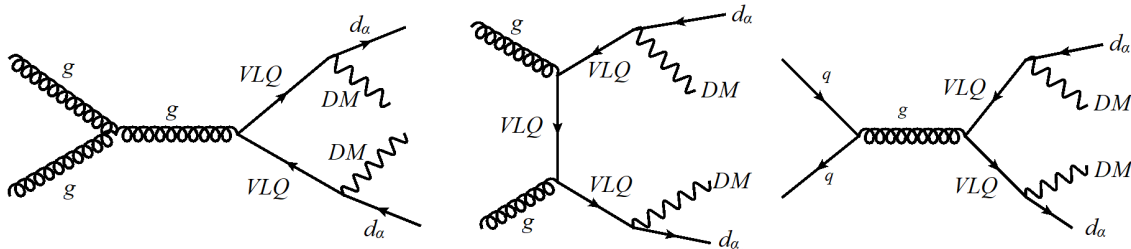


Figure 3: Representative Feynman diagrams for dominant vector like quark productions and subsequent decays at the LHC.

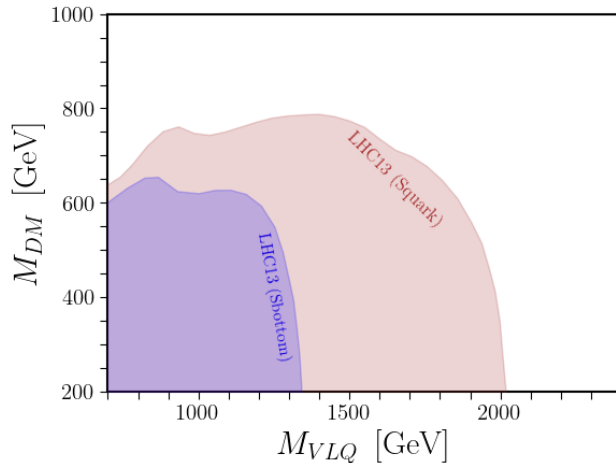


Figure 4: Current LHC limits on vector like quarks in our model.

Unlike vector-like lepton pair production, vector-like quark pair production at the LHC will be dominated by gluon-gluon fusion processes. Representative Feynman diagrams for the dominant production processes are shown in Fig. 3. The vector-like quark pair production rate is exclusively dictated by the strong coupling and vector-like quark masses. In our model, vector-like quarks decay to vector boson dark matter along with down-type quarks. This will result in $pp \rightarrow jj + \cancel{E}_T$ and $pp \rightarrow b\bar{b} + \cancel{E}_T$ signatures. In

supersymmetry, squark or gluino can lead to the identical final state signatures, and there are specific experimental searches [36, 37] looking at $pp \rightarrow jj + \cancel{E}_T$ and $pp \rightarrow b\bar{b} + \cancel{E}_T$ signatures. It is worth noting that the rates of squark or gluino creation differ significantly from the rates of vector-like quark pair formation. We compute the production rate using `MadGraph5aMC@NLO` [35] and recast the limit from supersymmetric squark searches [36] by comparing the signal cross-sections to the experimental upper bounds on the cross-sections assuming the cut efficiencies are identical in both scenarios. We find that the bound on vector-like quarks leading to the $pp \rightarrow jj + \cancel{E}_T$ signature is ~ 2 TeV, whereas the bound on vector-like quarks leading to the $pp \rightarrow b\bar{b} + \cancel{E}_T$ signature is 1.3 TeV. All these limits on vector-like quarks are summarized in Fig. 4. It should be noted that vector-like quarks can be created individually via quark-gluon fusion processes, resulting in a monojet signature in conjunction with missing energy. The single production rate of vector-like quarks is affected by both the gauge coupling g_R and the strong coupling constant. We find that the single production rate is significantly suppressed, and the limit from the pair-production scenario is stronger than the single production case. It can be foreseen that the next collider experiments like the HL-LHC, HE-LHC, and FCC-hh will provide ample opportunity to test this vector-like fermion portal dark matter scenario in its complete range.

4 Vector Boson Dark Matter Phenomenology

In this section we analyze the allowed parameter space of the vector boson DM by numerically evaluating the relic abundance of the DM using the software `MicrOmegas` [38, 39]. The model is implemented in `CalcHEP` [40] by using `LanHEP` [41]. In the limit of $(V_N - V_\nu) = aV_n$, with $V_n \ll V_N$ and a being order one, the mass of dark matter W_{7R} from Eq. (2.17) reads as

$$M_{W_{7R}} \equiv M_{DM} \simeq \frac{1}{\sqrt{2}} g_R V_n \sqrt{1 + 2a^2}. \quad (4.1)$$

Moreover, since the DM mass and exotic-fermion masses are controlled by the same $U(1)$ breaking VEV V_n , one can obtain theoretical limit on the ratio of DM mass and vector-like fermion mass. Using this equation together with Eq. (2.4) or Eq. (2.5) and demanding Yukawa $Y \leq 1.5$ (which is the perturbative unitarity limit), one obtains

$$M_{VLQ} \leq \frac{5M_{DM}}{\sqrt{1 + a^2}}. \quad (4.2)$$

This sets a strong theoretical bound in the model parameters, making the model very predictive, as discussed below. It is important to stress that to avoid the DM decay into exotic plus a SM fermions, the mass of the DM should obey $M_{DM} < M_{VLQ}, M_{VLL}$, where VLQ (VLL) stands for vector-like quarks (leptons).

4.1 Annihilation cross section and relic abundance

The relic density of DM is achieved through standard thermal freeze-out mechanism. Pairs of dark matter can annihilate through the three point and four point couplings as shown in

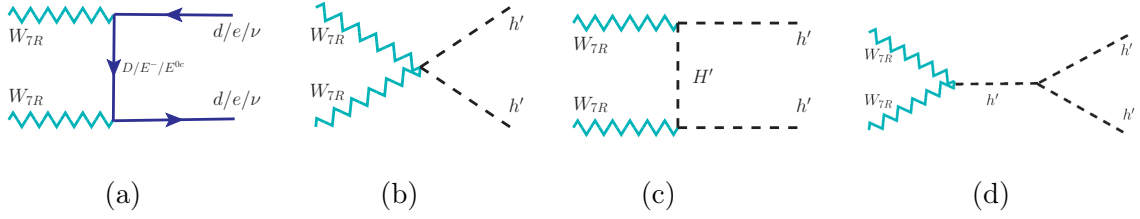


Figure 5: Relevant Feynman diagrams that contribute to vector DM annihilation.

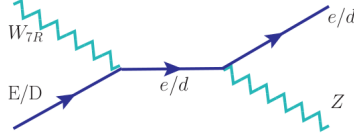


Figure 6: A typical Feynman diagram that contribute to co-annihilation of DM. There is an additional diagram with exotic charged lepton E replaced by E^{c0} and SM charged lepton replaced by neutrinos. Furthermore there are diagrams with Z replaced by W^\pm and gluons with corresponding fermions.

Fig. 5 mediated by an off- or on-shell scalar bosons or exotic fermions. The relevant gauge interactions of DM with the light degrees that are used for annihilation are given by

$$\begin{aligned} \mathcal{L} \supset & \frac{g_R}{2} W_{7R}^\mu \left[i(E^- \bar{e}^- + \bar{\nu} E^{c0} + d_R \bar{D}_R + h.c.) + (h' \partial_\mu H' - H' \partial_\mu h') \right] \\ & + \frac{g_R^2}{8} W_{7R}^\mu W_{7R\mu} (h' h' + H' H'). \end{aligned} \quad (4.3)$$

As already mentioned, the scalar fields that can be light in the framework are T -even neutral scalars h' and \tilde{h} , a doubly charged scalar δ^{++} , and T -odd neutral scalar H' , whose masses are given in Eq. (A.20), Eq. (A.16), and Eq. (A.56) respectively. For simplicity, we take masses of \tilde{h} , H' and δ^{++} heavier than the vector boson DM. Such a choice is consistent within our model as shown by Table. I. With this simplification, a pair of DM can annihilate to (i) SM fermion pair ($d\bar{d}$, $e\bar{e}$, $\nu\bar{\nu}$) via the exchange of exotic fermions (D_R , E^- , E^{c0}) through t -channel graph as shown in Fig. 5 (a), (ii) a pair of h' via the exchange of H' , h and through four point contact term as shown in Fig. 5 (b)-(d), and (iii) pairs of SM particles through the mixing between h' and SM Higgs h . The mixing between h' and SM Higgs is heavily constrained by DM direct detection constraints [42–45]. Here we turn off such couplings and avoid the constraint from direct detection. It is also important to note that if T -parity odd exotic fermions mass is close to the DM mass, it can contribute to co-annihilation, which would can have strong impact on the relic abundance in the model. A typical graph for co-annihilation is shown in Fig. 6.

All the relevant couplings for the annihilation are determined by the gauge coupling g_R given in Eq. (4.3) except for the diagram in Fig. 5 (d), where the vertices are $\frac{g_R^2 V_n}{2\sqrt{2}} (W_{7R} W_{7R} h')$ and $\sqrt{2} \lambda_{h'} V_n (h'^3)$. The VEV V_n can be traded off for the mass of DM given in Eq. (4.1), whereas the quartic coupling λ' is given by Eq. (A.24). Thus the effective parameters that

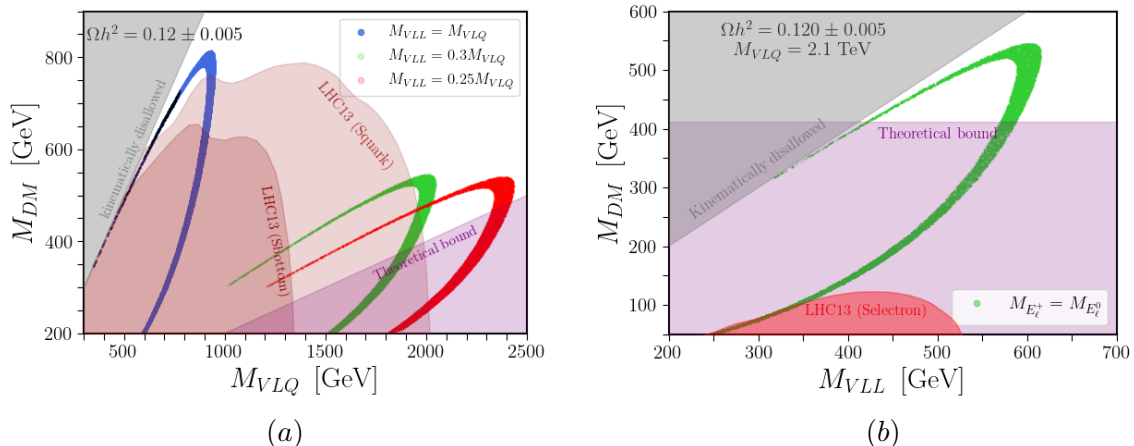


Figure 7: Allowed regions in the mass of dark matter M_{DM} and mass of vector-like fermion $M_{VLQ}(M_{VLL})$ plane that satisfy relic abundance requirement. The T -even h' and T -odd H' scalar masses are taken much heavier than the mass of vector-like fermions here, so that only t -channel process as shown in Fig. 5 (a) contributes. The gray and purple shaded regions are respectively from kinematically disallowed ($M_{DM} > M_{VLQ}$) region and theoretical bound ($M_{VLQ} > 5M_{DM}$). In the left panel (blue, green, red) shades respectively represents allowed parameter space that satisfies the relic abundance for the choice of ratio of mass of $M_{VLL}/M_{VLQ} = (1, 0.3, 0.25)$. Dark (light) brown corresponds to the exclusion region from $pp \rightarrow jj(bb) + \cancel{E}_T$ obtained by recasting the supersymmetric squark (sbottom) searches. The black segment along the abundance curve is excluded from direct detection constraints [43]. In the right panel the green band corresponds to the allowed parameter space that satisfies the relic abundance for a fixed VLQ mass 2.1 TeV. The red band is the exclusion region from $pp \rightarrow l^+l^- + \cancel{E}_T$ signature obtained by recasting supersymmetric slepton searches.

characterizes the relic abundance of DM in the model are:

$$\{M_{DM}, M_{VLQ}, M_{VLL}, M_{h'}\}, \quad (4.4)$$

where we take the masses for all three fermions to be equal. Note that the gauge coupling g_R at energy scale 2 TeV is 0.445. The running of g_R does not effect the phenomenology by much as the change in g_R is very small when running from 1 TeV to 10^3 TeV. To explore the parameter space, we adopt two scenarios: (i) $M_{h'} > M_{DM}$, such that only t -channel graph via the exchange of vector-like fermions in Fig. 5 (a) contributes, and (ii) $M_{h'}$ fixed at a particular value such that when $M_{DM} > M_{h'}$ new annihilation modes open up as shown in Fig. 5 (b)-(d). It is important to point out that there are no allowed parameter space while only considering annihilation mode to a pair of h' , as one cannot take the mass of vector-like fermion much bigger than DM mass.

For the first case with t -channel annihilation of DM into SM fermions, the relevant parameters are $\{M_{DM}, M_{VLQ}, M_{VLL}\}$. Here we explore two scenarios: (i) taking the

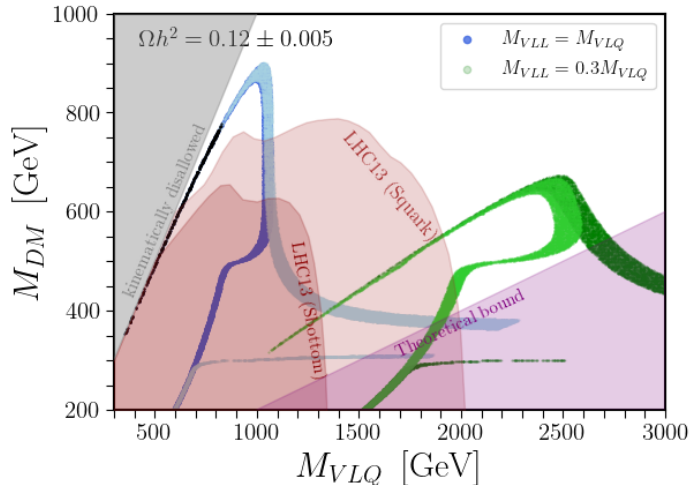


Figure 8: Allowed regions in the mass of dark matter M_{DM} and mass of exotic quark plane that satisfies relic abundance. The T -even h' scalar masses is kept at fixed value such that when $M_{DM} > M_{h'}$, all the annihilation modes of in Fig. 5 are relevant. Light (dark) blue band corresponds to allowed parameter space with $M_{VLL} = M_{VLQ}$ that satisfies relic density for $M_{h'} = 300$ (500) GeV, whereas light (dark) green represents for $M_{VLL} = 0.3 M_{VLQ}$ for $M_{h'} = 300$ (500) GeV. The black segment along the abundance curve is excluded from direct detection constraints [43].

ratio of VLQ and VLL fixed and varying mass of DM and VLQ, depicted in Fig 7 (a), and (ii) fixing $M_{VLQ} = 2.1$ TeV so that the collider bounds are satisfied and varying in the plane of DM mass and VLL mass, which is depicted in Fig 7 (b). The color shaded regions are the excluded in Fig 7. The gray and purple shaded regions are excluded respectively from kinematically disallowed ($M_{DM} > M_{VLQ}$) regions and theoretical bound ($M_{VLQ} > 5M_{DM}$). In Fig 7 (a), (blue, green, red) regions respectively represent allowed parameter space that satisfies the relic abundance $\Omega h^2 = 0.12 \pm 0.005$ for the choice of ratio of mass of $M_{VLL}/M_{VLQ} = (1, 0.3, 0.25)$. Dark (light) brown corresponds to the exclusion region from $pp \rightarrow jj(bb) + \cancel{E}_T$ obtained by recasting the supersymmetric squark (sbottom) searches. Note that choosing other ratios such as $M_{VLL} > M_{VLQ}$ ($M_{VLL} \lesssim 0.2M_{VLQ}$) is excluded by squark searches (theoretical limit). Thus, a very narrow parameter space is allowed which could be probed/excluded by the future colliders such as HL-LHC and FCC-hh.

Similarly in Fig 7 (b), the green band corresponds to the allowed parameter space that satisfies the relic abundance constraint. We fix the VLQ mass at 2.1 TeV, as heavier masses would only make the theoretical constraint stronger, thus decreases the allowed parameter space. Here all the vector-like lepton masses are taken to be degenerate. The red band is the exclusion region from $pp \rightarrow l^+l^- + \cancel{E}_T$ signature obtained by recasting supersymmetric slepton searches. We find that DM mass from 400 – 550 GeV is allowed in this scenario. The thin band where DM mass is close to vector-like fermion mass in both the figures corresponds to the contribution coming dominantly from co-annihilation.

The parameter space discussed above can be slightly improved by including all the annihilation modes of Fig. 5. We fix the mass of the T -even SM singlet Higgs field h' at (0.3, 0.5) TeV such that when $M_{DM} > M_{h'}$, pairs of DM can annihilate into pairs of h' (we keep \tilde{h} field to be heavy here). Fig. 8 shows the allowed parameter space that satisfies relic density including various theoretical and experimental bounds discussed earlier. The dark (light) blue band corresponds to the case when $M_{VLL} = M_{VLQ}$ for the choice of $M_{h'} = 0.5$ (1.0) TeV. As is clear from the figure, DM mass is improved to ~ 0.9 TeV compared to ~ 0.8 TeV from Fig. 7. Similarly, by taking the ratio of $M_{VLL}/M_{VLQ} = 0.3$, an improvement on DM mass from 550 GeV to 670 GeV is achieved as shown by the green band in Fig. 8. We have verified that each of these numerical solutions is consistent with an approximate analytical solution given in Ref. [46] for real vector DM at low relative velocity. We conclude that vector boson DM is consistent within the trinification model when its mass is less than 900 GeV. This corresponds to a theoretical bound on both vector-like quarks and leptons of 4.5 TeV.

Spin-independent direct DM-nucleon cross-section for vector boson DM at tree level [25, 47, 48] can in principle give a stringent constraint on the parameter space of the model. The t -channel diagrams which can potentially give large contribution to direct detection cross sections is subdominant in the limit of tiny mixing between SM higgs and weak-singlet higgs h' . Tree-level diagrams of weak-singlets color triplet fermions D_R exchange can generate interaction of vector boson dark matter with quarks which can constrain the parameter space discussed before. However, we find that the cross sections are far below the exclusion limit for almost all the parameter space, except in the s -channel ($M_{DM} \sim m_{VLQ}$). The exclusion is depicted as a black band overlaid on top of relic density plot in Fig. 7 and Fig. 8. Note that the loop contributions to direct detection amplitudes via penguin diagram with the exchange of Z/γ and vector dark matter coupling to gluons via box diagrams can be important, which is beyond the scope of the present work.

5 Conclusion

We have developed in this paper plausible dark matter candidates arising from TeV scale trinification theories. Symmetry breaking can be achieved while preserving a trinification parity (T -parity). Under this parity, the SM fermions are all even, while the vector-like quarks and leptons present in the theory are odd. Among the new gauge bosons some are T -even while some are T -odd. This setup admits singlet-doublet DM candidate, as well as a scalar singlet DM candidate.

The main focus of the paper has been the identification of a T -odd vector boson as the DM candidate. It has off-diagonal couplings connecting SM fermions and vector-like fermions. We have analyzed the DM phenomenology of this setup. LHC searches for dilptons with missing energy as well as dijet with missing energy provide strong constraints on the model parameters. We have shown consistent parameter space which satisfies these limits while being consistent with relic abundance and direct DM detection limits. The model predicts the vector boson DM mass to be below 900 GeV, along with upper limits

of 4.5 TeV on the vector-like quark and lepton masses. The entire parameter space of the model should be explored in future collider experiments.

Acknowledgement

The work of KSB is supported by the US Department of Energy Grant No. DE-SC 0016013.

A Appendix

Here we explicitly work out the scalar spectrum of the model in the electroweak preserving limit as discussed in Sec. 2.3. There are 36 components in the $\chi_{ij}^{\alpha\beta}$ fields which decomposes into 6 triplets, 6 doublets, and 6 singlets fields, whereas Φ_i^α decomposes into 3 doublets and 3 singlet fields under $SU(2)_L$.

A.1 T -parity even fields

A.1.1 Weak-triplet scalars

The T -parity even weak triplets defined in Eq. (1.1) have the field composition given by

$$\chi_{EE} (1, 3, 1) = \begin{pmatrix} \chi_{22}^{11} \\ \chi_{12}^{11} \\ \chi_{11}^{11} \end{pmatrix}, \quad \chi_{EE^c} (1, 3, 1) = \begin{pmatrix} \chi_{11}^{22*} \\ \chi_{12}^{22*} \\ \chi_{22}^{22*} \end{pmatrix}, \quad \chi_{e\nu} (1, 3, 1) = \begin{pmatrix} \chi_{11}^{33*} \\ \chi_{12}^{33*} \\ \chi_{22}^{33*} \end{pmatrix}. \quad (\text{A.1})$$

The weak state $(\chi_{EE}^i, \chi_{EE^c}^i, \chi_{e\nu}^i)$ mix to form a 3×3 matrix. The elements of the mass-squared matrix M_{ij} in this basis read as

$$\begin{aligned} M_{11} &= -\lambda_{10}V_n^2 - 2(\lambda_3 + \lambda_4)V_N^2 - 2(\lambda_2 + \lambda_3 + \lambda_4 + \lambda_5)V_\nu^2 \\ M_{22} &= -\lambda_{10}V_n^2 - 2(\lambda_3 + \lambda_4)V_N^2 - 2(\lambda_4 + \lambda_5)V_\nu^2 \\ M_{22} &= (\lambda_9 - \lambda_{10})V_n^2 + 2(\lambda_2 - \lambda_4)V_N^2 - 2(\lambda_2 + \lambda_3 + \lambda_4 + \lambda_5)V_\nu^2 \\ M_{12} &= 2\lambda_{14}V_n^2 + 6\mu_\chi V_N \\ M_{13} &= 6\mu_\chi V_\nu \\ M_{23} &= 2\lambda_3 V_N V_\nu \end{aligned} \quad (\text{A.2})$$

For the benchmark values given in Table I, these squared masses are all positive and the masses normalized to V_N are respectively $\{3.62, 2.80, 0.96\}$ and $\{2.86, 2.42, 1.70\}$ for BP-I and BP-II.

A.1.2 Weak-doublet scalars

The four T -parity even doublets have the composition given as follows:

$$\chi_{EN} (1, 2, 1/2) = \begin{pmatrix} \chi_{23}^{13} \\ \chi_{13}^{13} \end{pmatrix}, \quad \chi_{E^cN} (1, 2, 1/2) = \begin{pmatrix} \chi_{13}^{23*} \\ \chi_{23}^{23*} \end{pmatrix}, \quad (\text{A.3})$$

$$\Phi_{EE^c} (1, 2, 1/2) = \begin{pmatrix} \Phi_1^{2*} \\ \Phi_2^{2*} \end{pmatrix}, \quad \Phi_{EE} (1, 2, 1/2) = \begin{pmatrix} \Phi_2^1 \\ \Phi_1^1 \end{pmatrix}. \quad (\text{A.4})$$

The weak state $(\chi_{EN}^i, \chi_{E^cN}^i, \Phi_{EE^c}^i, \Phi_{EE}^i)$ mix to form a 4×4 matrix. The elements of the squared mass matrix, constructed from the bilinear terms by expanding the potential about its minimum, denoted as \tilde{M}_{ij} , read as

$$\begin{aligned} \tilde{M}_{11} = & \frac{1}{4}(-2\lambda_{10} + \lambda_{11} + 2\lambda_9)V_n^2 + (\lambda_2 - 2\lambda_3 - \lambda_4 + \lambda_5)V_N^2 \\ & - (2\lambda_2 + 2\lambda_3 + \lambda_4 + 2\lambda_5)V_\nu^2 \end{aligned} \quad (\text{A.5})$$

$$\begin{aligned} \tilde{M}_{22} = & \frac{1}{4}(-2\lambda_{10} + \lambda_{11} + 2\lambda_9)V_n^2 + (\lambda_2 - 2\lambda_3 - \lambda_4 + \lambda_5)V_N^2 \\ & - (\lambda_2 + 2\lambda_3 + \lambda_4 + \lambda_5)V_\nu^2 \end{aligned} \quad (\text{A.6})$$

$$\begin{aligned} \tilde{M}_{33} = & -2\lambda_7V_n^2 + (-\lambda_{10} + \lambda_{11} + \lambda_9)V_N^2 + (-\lambda_{10} + \lambda_9)V_\nu^2 \\ & + \frac{4}{V_n^2}(\lambda_2 + \lambda_5)V_N^2(V_N^2 - V_\nu^2) \end{aligned} \quad (\text{A.7})$$

$$\begin{aligned} \tilde{M}_{44} = & -2\lambda_7V_n^2 - \lambda_{10}(V_N^2 + V_\nu^2) + V_n^2[\lambda_{11} + \lambda_9 \\ & + \frac{4}{V_n^2}(\lambda_2 + \lambda_5)(V_N^2 - V_\nu^2)] \end{aligned} \quad (\text{A.8})$$

$$\tilde{M}_{12} = -\frac{1}{2}\lambda_{12}V_nV_N \quad (\text{A.9})$$

$$\tilde{M}_{13} = -\lambda_{13}V_n^2 - \lambda_{12}V_N^2 \quad (\text{A.10})$$

$$\tilde{M}_{14} = -\frac{1}{2}\lambda_{11}V_nV_N - \lambda_9V_nV_N - \frac{2}{V_n}(\lambda_2 + \lambda_5)V_N(V_N^2 - V_\nu^2) \quad (\text{A.11})$$

$$\tilde{M}_{23} = -\frac{1}{2}\lambda_{11}V_nV_N - \lambda_9V_nV_N - \frac{2}{V_n}(\lambda_2 + \lambda_5)V_N(V_N^2 - V_\nu^2) \quad (\text{A.12})$$

$$\tilde{M}_{24} = -\lambda_{13}V_n^2 + \lambda_{12}(-V_N^2 + V_\nu^2) \quad (\text{A.13})$$

$$\tilde{M}_{34} = -V_n(\mu_\phi + 2\lambda_{13}V_N) \quad (\text{A.14})$$

The mass-squared values of these T -even doublets are all positive and the masses normalized to V_N for benchmark BP-I and BP-II are $\{2.86, 2.53, 2.21, 2.02\}$ and $\{2.72, 2.36, 1.83, 1.64\}$, respectively.

A.1.3 Weak-singlet scalars

The five T -even singlet fields are given by

$$\chi_{33}^{11} (1, 1, 2), \quad \chi_{33}^{12} (1, 1, 1), \quad \chi_{33}^{22} (1, 1, 0), \quad \chi_{33}^{33} (1, 1, 0), \quad \Phi_3^3 (1, 1, 0). \quad (\text{A.15})$$

The singly charged field χ_{33}^{12} is a Goldstone mode. The mass of the doubly charged χ_{33}^{11} field reads as

$$M_{\chi_{33}^{11}}^2 = -2V_\nu^2(\lambda_2 + \lambda_5). \quad (\text{A.16})$$

Notice that $(\lambda_2 + \lambda_5) < 0$ is required for this mass parameter to be positive, which is satisfied in the two benchmark points which correspond to mass eigenvalues given for BP-I (BP-II) are $0.133 V_N$ ($0.118 V_N$).

There is a mixing between $\{\text{Re}[\chi_{33}^{22}], \text{Re}[\chi_{33}^{33}], \text{Re}[\Phi_3^3]\}$ fields and the matrix elements are given by

$$M_{11} = 4(\lambda_1 + \lambda_2 + \lambda_3 + \lambda_4 + \lambda_5)V_\nu^2 \quad (\text{A.17})$$

$$M_{22} = (\lambda_{11} + \lambda_9)V_n^2 + 2[2\lambda_1 + 3\lambda_2 + 2(\lambda_3 + \lambda_4) + 3\lambda_5]V_N^2 \quad (\text{A.18})$$

$$M_{33} = 4(\lambda_6 + \lambda_7)V_n^2 \quad (\text{A.19})$$

$$M_{12} = 4(\lambda_1 + \lambda_3 + \lambda_4)V_N V_\nu \quad (\text{A.20})$$

$$M_{13} = 2(\lambda_{10} + \lambda_8)V_n V_\nu \quad (\text{A.21})$$

$$M_{23} = 2(\lambda_{10} + \lambda_8)V_n V_N - \frac{4V_N}{V_n}(\lambda_2 + \lambda_5)(V_N^2 - V_\nu^2). \quad (\text{A.22})$$

The eigenvalues of the the above 3×3 mass matrix are positive and the masses normalized to V_N are given as $\{1.30, 0.65, 0.057\}$ and $\{1.60, 0.39, 0.095\}$ for BP-I and BP-II, respectively. The lightest field is identified as h' , relevant for DM analysis. In the limit $\text{Re}[\Phi_3^3]$ mixing with $\text{Re}[\chi_{33}^{22}]$, $\text{Re}[\chi_{33}^{33}]$ small, the mass of the $\text{Re}[\Phi_3^3]$ is simply given as

$$M_{h'} \simeq 2\sqrt{\lambda_{h'}} V_n, \quad (\text{A.23})$$

which allows the quartic coupling of the interaction $\frac{\lambda_{h'}}{4} (h'h'^*)^2$, essential for pair of DM annihilation to pair of h' , to be written as

$$\lambda_{h'} = \frac{g_R^2}{8} \frac{M_{h'}^2 (1 + 2a^2)}{M_{W_7}^2}. \quad (\text{A.24})$$

The neutral field $\text{Im}[\chi_{33}^{22}]$ is a Goldstone modes. The neutral field $\{\text{Im}[\chi_{33}^{33}], \text{Im}[\Phi_3^3]\}$ mix to give a Goldstone mode and a physical state:

$$G''^0 = \frac{2V_N \text{Im}[\chi_{33}^{33}] + V_n \text{Im}[\Phi_3^3]}{\sqrt{V_n^2 + 4V_N^2}} \quad (\text{A.25})$$

$$X''^0 = \frac{-V_n \text{Im}[\chi_{33}^{33}] + 2V_N \text{Im}[\Phi_3^3]}{\sqrt{V_n^2 + 4V_N^2}} \quad (\text{A.26})$$

where G''^0 is a Goldstone mode, and X''^0 is the orthogonal state with the physical mass given by

$$M_{X''^0}^2 = \frac{1}{V_n^2} (V_n^2 + 4V_N^2) [(\lambda_{11} + \lambda_{19})V_n^2 + 2(\lambda_2 + \lambda_5)(V_N^2 - V_\nu^2)]. \quad (\text{A.27})$$

The mass-squared corresponding to Eq. (A.27) is positive and the mass of this T -even neutral field $(1, 1, 0)$ is $3.75 V_N$ for TX-I and $3.80 V_N$ for TX-II.

A.2 T -parity odd fields

A.2.1 Weak-triplet scalars

The three T -parity odd triplets are given as follows:

$$\chi_{Ee} (1, 3, 1) = \begin{pmatrix} \chi_{11}^{23*} \\ \chi_{12}^{23*} \\ \chi_{22}^{23*} \end{pmatrix}, \quad \chi'_{EE} (1, 3, 0) = \begin{pmatrix} \chi_{11}^{12*} \\ \chi_{12}^{12*} \\ \chi_{22}^{12*} \end{pmatrix}, \quad \chi'_{E\nu} (1, 3, 0) = \begin{pmatrix} \chi_{11}^{13*} \\ \chi_{12}^{13*} \\ \chi_{22}^{13*} \end{pmatrix}. \quad (\text{A.28})$$

The mass for the triplets χ_{Ee} reads as

$$M_{\chi_{Ee}}^2 = \frac{1}{2} (\lambda_9 - 2\lambda_{10})V_n^2 + (\lambda_2 - 2(\lambda_3 + \lambda_4))V_N^2 - (\lambda_2 + 2(\lambda_3 + \lambda_4 + \lambda_5))V_\nu^2. \quad (\text{A.29})$$

The neutral fields χ_{12}^{12} and χ_{12}^{13} have the following masses:

$$M_{(\text{Re,Im})[\chi_{12}^{12}]}^2 = (-\lambda_{10} + 2\lambda_{14})V_n^2 \pm 6\mu_\chi V_N - 2(\lambda_3 + \lambda_4)V_N^2 - (\lambda_2 + 2(\lambda_3 + \lambda_4 + \lambda_5))V_\nu^2, \quad (\text{A.30})$$

$$M_{(\text{Re,Im})[\chi_{12}^{13}]}^2 = \frac{1}{2}(\lambda_9 - 2\lambda_{10})V_n^2 \pm 6\mu_\chi V_\nu + (\lambda_2 - 2(\lambda_3 + \lambda_4))V_N^2 - 2(\lambda_2 + \lambda_3 + \lambda_4 + \lambda_5)V_\nu^2. \quad (\text{A.31})$$

The fields $\{\chi_{11}^{12*}, \chi_{22}^{12}\}$ and $\{\chi_{11}^{13*}, \chi_{22}^{13}\}$ mix to form 2×2 matrices. The eigenstates corresponding to these matrices are

$$X_\pm = \frac{1}{\sqrt{2}}(\chi_{22}^{12} \pm \chi_{11}^{12*}), \quad (\text{A.32})$$

$$X'_\pm = \frac{1}{\sqrt{2}}(\chi_{22}^{13} \pm \chi_{11}^{13*}). \quad (\text{A.33})$$

The masses corresponding to the physical state X_\mp and X'_\mp are respectively given by Eqs. (A.30) and (A.31). For the benchmark values given in Table I, the mass-squared values are positive and the masses for the fields $\{M_{\chi_{Ee}}, M_{\text{Re}[\chi_{12}^{12}]}, M_{\text{Im}[\chi_{12}^{12}]}, M_{\text{Re}[\chi_{12}^{13}]}, M_{\text{Im}[\chi_{12}^{13}]}\}$ normalized to V_N are respectively $\{2.80, 1.81, 3.50, 1.98, 3.43\}$ and $\{2.42, 1.96, 2.77, 2.03, 2.75\}$ for BP-I and BP-II.

A.2.2 Weak-doublet scalars

There is a $(1, 2, 3/2)$ multiplet given by

$$\chi_{Eec} (1, 2, 3/2) = \begin{pmatrix} \chi_{23}^{11} \\ \chi_{13}^{11} \end{pmatrix}. \quad (\text{A.34})$$

The mass for the above T - odd doublet reads as

$$M_{\chi_{Eec}}^2 = -\frac{1}{2}\lambda_{10}V_n^2 - (2\lambda_3 + \lambda_4)V_N^2 - (2\lambda_2 + 2\lambda_3 + \lambda_4 + 2\lambda_5)V_\nu^2. \quad (\text{A.35})$$

The mass-squared of this scalar field is positive and the mass for the BP-I is $2.19V_N$ and $1.80V_N$ for BP-II. The four T -parity odd doublets that mix with each other are

$$\chi_{E\nu^c} (1, 2, 1/2) = \begin{pmatrix} \chi_{23}^{12} \\ \chi_{13}^{12} \end{pmatrix}, \quad \chi_{E^c\nu^c} (1, 2, 1/2) = \begin{pmatrix} \chi_{13}^{22*} \\ \chi_{23}^{22*} \end{pmatrix}, \quad (\text{A.36})$$

$$\chi_{eN} (1, 2, 1/2) = \begin{pmatrix} \chi_{13}^{33*} \\ \chi_{23}^{33*} \end{pmatrix}, \quad \Phi_{e\nu} (1, 2, 1/2) = \begin{pmatrix} \Phi_1^{3*} \\ \Phi_2^{3*} \end{pmatrix}. \quad (\text{A.37})$$

The weak state $(\chi_{E\nu^c}^i, \chi_{E^c\nu^c}^i, \chi_{eN}^i, \Phi_{e\nu}^i)$ mix to form a 4×4 matrix. The elements of the mass spectrum \hat{M}_{ij} read as

$$\hat{M}_{11} = -\frac{1}{2}\lambda_{10}V_n^2 - (2\lambda_3 + \lambda_4)V_N^2 - (\lambda_2 + 2\lambda_3 + \lambda_4 + \lambda_5)V_\nu^2 \quad (\text{A.38})$$

$$\hat{M}_{22} = -\frac{\lambda_{10}}{2}V_n^2 - 2(\lambda_3 + \lambda_4)V_N^2 \quad (\text{A.39})$$

$$\hat{M}_{33} = \frac{V_n^2}{2}(-\lambda_{10} + \lambda_{11} + 2\lambda_9) + 2(\lambda_2 + \lambda_5)V_N^2 - (2\lambda_2 + 2\lambda_3 + \lambda_4 + 2\lambda_5)V_\nu^2 \quad (\text{A.40})$$

$$\hat{M}_{44} = -\lambda_{10}(V_N^2 + V_\nu^2) + V_N^2[\lambda_{11} + 2\lambda_9 + \frac{4}{V_n^2}(\lambda + 2 + \lambda_5)(V_N^2 - V_\nu^2)] \quad (\text{A.41})$$

$$\hat{M}_{12} = -\frac{\lambda_{12}}{\sqrt{2}}V_n V_\nu \quad (\text{A.42})$$

$$\hat{M}_{13} = 0 \quad (\text{A.43})$$

$$\hat{M}_{14} = \lambda_{12}V_\nu^2 \quad (\text{A.44})$$

$$\hat{M}_{23} = (2\lambda_3 + \lambda_4)V_N V_\nu \quad (\text{A.45})$$

$$\hat{M}_{24} = \frac{\lambda_{10}}{\sqrt{2}}V_n V_\nu \quad (\text{A.46})$$

$$\hat{M}_{34} = \frac{V_n V_N}{\sqrt{2}}[\lambda_{10} - \lambda_{11} - 2\lambda_9 - \frac{4}{V_n^2}(\lambda_2 + \lambda_5)(V_N^2 - V_\nu^2)] . \quad (\text{A.47})$$

There are two Goldstone modes associated with the doublets fields given in Eq. (A.36) and Eq. (A.37):

$$G^+ = \frac{\sqrt{2}V_\nu\chi_{13}^{22*} + \sqrt{2}V_N\chi_{13}^{33*} + V_n\Phi_1^{3*}}{\sqrt{V_n^2 + 2(V_N^2 + V_\nu^2)}} , \quad (\text{A.48})$$

$$G^0 = \frac{\sqrt{2}V_\nu\chi_{23}^{22} + \sqrt{2}V_N\chi_{23}^{33} + V_n\Phi_2^3}{\sqrt{V_n^2 + 2(V_N^2 + V_\nu^2)}} . \quad (\text{A.49})$$

The masses of the T -parity odd scalar field (1,2,1/2) for the BP-I is {2.93, 2.21, 2.10} V_N and {2.78, 1.83, 1.71} V_N for BP-II, with all eigenvalues being positive.

A.2.3 Weak-singlet scalars

The T -odd singlet fields are

$$\chi_{33}^{13} (1, 1, 1), \quad \chi_{33}^{23} (1, 1, 0), \quad \Phi_3^1 (1, 1, 1), \quad \Phi_3^2 (1, 1, 0). \quad (\text{A.50})$$

The singly charged singlet fields $\{\chi_{33}^{13}, \Phi_3^1\}$ mix to give one physical state and a Goldstone mode:

$$G'^+ = \frac{\sqrt{2}V_N\chi_{33}^{13} + V_n\Phi_3^1}{\sqrt{V_n^2 + 2V_N^2}} \quad (\text{A.51})$$

$$X'^+ = \frac{-V_n\chi_{33}^{13} + \sqrt{2}V_N\Phi_3^1}{\sqrt{V_n^2 + 2V_N^2}} \quad (\text{A.52})$$

The mass of the physical state X'^+ is given by

$$M_{X'^+}^2 = \frac{1}{2V_n^2}(V_n^2 + 2V_N^2)[(\lambda_{11} + \lambda_9)V_n^2 + 4(\lambda_2 + \lambda_5)(V_N^2 - V_\nu^2)] . \quad (\text{A.53})$$

The mass of the singly charged T -odd field (1, 1, 1) is 1.84 V_N (1.88 V_N) for BP-I (BP-II) with positive eigenvalue. The neutral fields $\{\text{Re}[\chi_{33}^{23}], \text{Re}[\Phi_3^2]\}$ mix to give one Goldstone modes.

$$G'^{0r} = \frac{\sqrt{2}(V_N - V_\nu)\text{Re}[\chi_{33}^{23}] + V_n\text{Re}[\Phi_3^2]}{\sqrt{V_n^2 + 2|V_N - V_\nu|^2}} \quad (\text{A.54})$$

$$X'^{0r} = \frac{-|V_N - V_\nu|V_n \text{Re}[\chi_{33}^{23}] + \sqrt{2}|V_N - V_\nu| \text{Re}[\Phi_3^2]}{\sqrt{V_n^2 + 2|V_N - V_\nu|^2}}. \quad (\text{A.55})$$

Here the mass of the physical state X'^{0r} is given by

$$M_{X'^{0r}}^2 = \frac{1}{2V_n^2} [V_n^2 + 2(V_N - V_\nu)^2] [(\lambda_{11} + \lambda_9)V_n^2 + 4V_N(\lambda_2 + \lambda_5)(V_N + V_\nu)]. \quad (\text{A.56})$$

As noted earlier, from the double charged scalar mass, $\lambda_2 + \lambda_5 < 0$ is required, which implies that $\lambda_2 + \lambda_5 = b (\lambda_9 + \lambda_{11}) V_n^2/V_N^2$ for the positivity of the mass squared term in Eq. (A.56). The mass of the neutral T -odd field ($\equiv H' \sim (1, 1, 0)$) is $0.165 V_N$ for BP-I and $0.187 V_N$ for BP-II with positive eigenvalue. Similarly, the neutral fields $\{\text{Im}[\chi_{33}^{23}], \text{Im}[\Phi_3^2]\}$ mix to give a Goldstone mode.

$$G'^{0i} = \frac{\sqrt{2}(V_N + V_\nu)\text{Im}[\chi_{33}^{23}] + V_n\text{Im}[\Phi_3^2]}{\sqrt{V_n^2 + 2|V_N + V_\nu|^2}} \quad (\text{A.57})$$

$$X'^{0i} = \frac{-|V_N + V_\nu|V_n \text{Re}[\chi_{33}^{23}] + \sqrt{2}|V_N + V_\nu| \text{Re}[\Phi_3^2]}{\sqrt{V_n^2 + 2|V_N + V_\nu|^2}}. \quad (\text{A.58})$$

The mass of the physical state with is given by

$$M_{X'^{0i}}^2 = \frac{1}{2V_n^2} [V_n^2 + 2(V_N + V_\nu)^2] [(\lambda_{11} + \lambda_9)V_n^2 + 4(\lambda_2 + \lambda_5)V_N(V_N - V_\nu)]. \quad (\text{A.59})$$

The squared mass corresponding to Eq. (A.59) is positive with the mass being $3.51 V_N$ for TX-I and $3.60 V_N$ for TX-II.

In order to make the DM mass light, $V_N - V_\nu$ has to be of order V_n in Eq. (2.17), which can be achieved by making an expansion on $V_N - V_\nu = aV_n$ to first order in the extremum conditions of the potential Eq. (2.36)-(2.38). This leads to the following conditions

$$\begin{aligned} m_\phi^2 &= 2\mu_{\phi\chi}V_N + (2\lambda_{10} + \lambda_{11} + 2\lambda_8 + \lambda_9)V_N^2, \\ m_\chi^2 &= 2(2\lambda_1 + \lambda_2 + 2\lambda_3 + 2\lambda_4 + \lambda_5)V_N^2 \end{aligned} \quad (\text{A.60})$$

These are the precisely the terms that have been eliminated using the extremum conditions.

References

- [1] A. de Rujula, H. Georgi, and S. L. Glashow, “in Fifth Workshop on Grand Unification, edited by K. Kang, H. Fried, and P. Frampton,” (*World Scientific, Singapore, 1984*).
- [2] K. S. Babu, X.-G. He, and S. Pakvasa, “Neutrino Masses and Proton Decay Modes in SU(3) X SU(3) X SU(3) Trinification,” *Phys. Rev. D* **33** (1986) 763.
- [3] J. Sayre, S. Wiesenfeldt, and S. Willenbrock, “Minimal trinification,” *Phys. Rev. D* **73** (2006) 035013, [arXiv:hep-ph/0601040](#).
- [4] J. Hetzel and B. Stech, “Low-energy phenomenology of trinification: an effective left-right-symmetric model,” *Phys. Rev. D* **91** (2015) 055026, [arXiv:1502.00919 \[hep-ph\]](#).
- [5] J. E. Kim, “Trinification with $\sin^2 \theta(W) = 3/8$ and seesaw neutrino mass,” *Phys. Lett. B* **591** (2004) 119–126, [arXiv:hep-ph/0403196](#).

- [6] G. M. Pelaggi, A. Strumia, and S. Vignali, “Totally asymptotically free trinification,” *JHEP* **08** (2015) 130, [arXiv:1507.06848 \[hep-ph\]](#).
- [7] K. S. Babu, B. Bajc, M. Nemevšek, and Z. Tavartkiladze, “Trinification at the TeV scale,” *AIP Conf. Proc.* **1900** no. 1, (2017) 020002.
- [8] T. Cohen, J. Kearney, A. Pierce, and D. Tucker-Smith, “Singlet-Doublet Dark Matter,” *Phys. Rev. D* **85** (2012) 075003, [arXiv:1109.2604 \[hep-ph\]](#).
- [9] L. Calibbi, A. Mariotti, and P. Tziveloglou, “Singlet-Doublet Model: Dark matter searches and LHC constraints,” *JHEP* **10** (2015) 116, [arXiv:1505.03867 \[hep-ph\]](#).
- [10] T. Abe and R. Sato, “Current status and future prospects of the singlet-doublet dark matter model with CP-violation,” *Phys. Rev. D* **99** no. 3, (2019) 035012, [arXiv:1901.02278 \[hep-ph\]](#).
- [11] B. Barman, D. Borah, P. Ghosh, and A. K. Saha, “Flavoured gauge extension of singlet-doublet fermionic dark matter: neutrino mass, high scale validity and collider signatures,” *JHEP* **10** (2019) 275, [arXiv:1907.10071 \[hep-ph\]](#).
- [12] P. S. B. Dev, R. N. Mohapatra, and Y. Zhang, “Heavy right-handed neutrino dark matter in left-right models,” *Mod. Phys. Lett. A* **32** (2017) 1740007, [arXiv:1610.05738 \[hep-ph\]](#).
- [13] J. M. Berryman, A. de Gouvêa, K. J. Kelly, and Y. Zhang, “Dark Matter and Neutrino Mass from the Smallest Non-Abelian Chiral Dark Sector,” *Phys. Rev. D* **96** no. 7, (2017) 075010, [arXiv:1706.02722 \[hep-ph\]](#).
- [14] T. Abe and K. S. Babu, “Simple Theory of Chiral Fermion Dark Matter,” *Phys. Rev. D* **103** no. 1, (2021) 015031, [arXiv:1912.11332 \[hep-ph\]](#).
- [15] M. Gonderinger, H. Lim, and M. J. Ramsey-Musolf, “Complex Scalar Singlet Dark Matter: Vacuum Stability and Phenomenology,” *Phys. Rev. D* **86** (2012) 043511, [arXiv:1202.1316 \[hep-ph\]](#).
- [16] L. Coito, C. Faubel, J. Herrero-Garcia, and A. Santamaria, “Dark matter from a complex scalar singlet: the role of dark CP and other discrete symmetries,” *JHEP* **11** (2021) 202, [arXiv:2106.05289 \[hep-ph\]](#).
- [17] M. Cirelli, N. Fornengo, and A. Strumia, “Minimal dark matter,” *Nucl. Phys. B* **753** (2006) 178–194, [arXiv:hep-ph/0512090](#).
- [18] J. Heck and S. Patra, “Minimal Left-Right Symmetric Dark Matter,” *Phys. Rev. Lett.* **115** no. 12, (2015) 121804, [arXiv:1507.01584 \[hep-ph\]](#).
- [19] M. Kadastik, K. Kannike, and M. Raidal, “Dark Matter as the signal of Grand Unification,” *Phys. Rev. D* **80** (2009) 085020, [arXiv:0907.1894 \[hep-ph\]](#). [Erratum: *Phys.Rev.D* **81**, 029903 (2010)].
- [20] Y. Mambrini, N. Nagata, K. A. Olive, J. Quevillon, and J. Zheng, “Dark matter and gauge coupling unification in nonsupersymmetric SO(10) grand unified models,” *Phys. Rev. D* **91** no. 9, (2015) 095010, [arXiv:1502.06929 \[hep-ph\]](#).
- [21] K. S. Babu, B. Bajc, and V. Susic. to be published; see talk by B. Bajc at SUSY 2021, Beijing, July 2021.
- [22] J. L. Diaz-Cruz and E. Ma, “Neutral SU(2) Gauge Extension of the Standard Model and a Vector-Boson Dark-Matter Candidate,” *Phys. Lett. B* **695** (2011) 264–267, [arXiv:1007.2631 \[hep-ph\]](#).

- [23] F. Chen, J. M. Cline, and A. R. Frey, “Nonabelian dark matter: Models and constraints,” *Phys. Rev. D* **80** (2009) 083516, [arXiv:0907.4746 \[hep-ph\]](#).
- [24] T. Abe, M. Fujiwara, J. Hisano, and K. Matsushita, “A model of electroweakly interacting non-abelian vector dark matter,” *JHEP* **07** (2020) 136, [arXiv:2004.00884 \[hep-ph\]](#).
- [25] B. Barman, S. Bhattacharya, S. K. Patra, and J. Chakraborty, “Non-Abelian Vector Boson Dark Matter, its Unified Route and signatures at the LHC,” *JCAP* **12** (2017) 021, [arXiv:1704.04945 \[hep-ph\]](#).
- [26] J. F. Donoghue and B. R. Holstein, “Strong bounds on weak couplings,” *Phys. Lett. B* **113** (1982) 382–386.
- [27] K. S. Babu, K. Fujikawa, and A. Yamada, “Constraints on left-right symmetric models from the process $b \rightarrow s \gamma$,” *Phys. Lett. B* **333** (1994) 196–201, [arXiv:hep-ph/9312315](#).
- [28] K. Hadeler, “On copositive matrices,” *Linear Algebra and its Applications* **49** (1983) 79–89.
- [29] K. G. Klimenko, “On Necessary and Sufficient Conditions for Some Higgs Potentials to Be Bounded From Below,” *Theor. Math. Phys.* **62** (1985) 58–65.
- [30] V. Silveira and A. Zee, “SCALAR PHANTOMS,” *Phys. Lett. B* **161** (1985) 136–140.
- [31] J. McDonald, “Gauge singlet scalars as cold dark matter,” *Phys. Rev. D* **50** (1994) 3637–3649, [arXiv:hep-ph/0702143](#).
- [32] CMS Collaboration, A. M. Sirunyan *et al.*, “Search for supersymmetric partners of electrons and muons in proton-proton collisions at $\sqrt{s} = 13$ TeV,” *Phys. Lett. B* **790** (2019) 140–166, [arXiv:1806.05264 \[hep-ex\]](#).
- [33] ATLAS Collaboration, “Search for direct stau production in events with two hadronic tau leptons in $\sqrt{s} = 13$ TeV pp collisions with the ATLAS detector,”.
- [34] N. D. Christensen and C. Duhr, “FeynRules - Feynman rules made easy,” *Comput. Phys. Commun.* **180** (2009) 1614–1641, [arXiv:0806.4194 \[hep-ph\]](#).
- [35] J. Alwall, R. Frederix, S. Frixione, V. Hirschi, F. Maltoni, O. Mattelaer, H. S. Shao, T. Stelzer, P. Torrielli, and M. Zaro, “The automated computation of tree-level and next-to-leading order differential cross sections, and their matching to parton shower simulations,” *JHEP* **07** (2014) 079, [arXiv:1405.0301 \[hep-ph\]](#).
- [36] ATLAS Collaboration, G. Aad *et al.*, “Search for squarks and gluinos in final states with jets and missing transverse momentum using 139 fb⁻¹ of $\sqrt{s} = 13$ TeV pp collision data with the ATLAS detector,” *JHEP* **02** (2021) 143, [arXiv:2010.14293 \[hep-ex\]](#).
- [37] CMS Collaboration, A. M. Sirunyan *et al.*, “Search for supersymmetry in proton-proton collisions at 13 TeV in final states with jets and missing transverse momentum,” *JHEP* **10** (2019) 244, [arXiv:1908.04722 \[hep-ex\]](#).
- [38] G. Bélanger, F. Boudjema, A. Pukhov, and A. Semenov, “micrOMEGAs4.1: two dark matter candidates,” *Comput. Phys. Commun.* **192** (2015) 322–329, [arXiv:1407.6129 \[hep-ph\]](#).
- [39] G. Belanger, A. Mjallal, and A. Pukhov, “Recasting direct detection limits within micrOMEGAs and implication for non-standard Dark Matter scenarios,” *Eur. Phys. J. C* **81** no. 3, (2021) 239, [arXiv:2003.08621 \[hep-ph\]](#).
- [40] A. Belyaev, N. D. Christensen, and A. Pukhov, “CalcHEP 3.4 for collider physics within and beyond the Standard Model,” *Comput. Phys. Commun.* **184** (2013) 1729–1769, [arXiv:1207.6082 \[hep-ph\]](#).

- [41] A. Semenov, “LanHEP — A package for automatic generation of Feynman rules from the Lagrangian. Version 3.2,” *Comput. Phys. Commun.* **201** (2016) 167–170, [arXiv:1412.5016 \[physics.comp-ph\]](#).
- [42] **SuperCDMS** Collaboration, D. Speller, “Dark matter direct detection with SuperCDMS Soudan,” *J. Phys. Conf. Ser.* **606** no. 1, (2015) 012003.
- [43] **XENON** Collaboration, E. Aprile *et al.*, “Dark Matter Search Results from a One Ton-Year Exposure of XENON1T,” *Phys. Rev. Lett.* **121** no. 11, (2018) 111302, [arXiv:1805.12562 \[astro-ph.CO\]](#).
- [44] **LUX-ZEPLIN** Collaboration, D. S. Akerib *et al.*, “Projected WIMP sensitivity of the LUX-ZEPLIN dark matter experiment,” *Phys. Rev. D* **101** no. 5, (2020) 052002, [arXiv:1802.06039 \[astro-ph.IM\]](#).
- [45] **PandaX-4T** Collaboration, Y. Meng *et al.*, “Dark Matter Search Results from the PandaX-4T Commissioning Run,” [arXiv:2107.13438 \[hep-ex\]](#).
- [46] A. Berlin, D. Hooper, and S. D. McDermott, “Simplified Dark Matter Models for the Galactic Center Gamma-Ray Excess,” *Phys. Rev. D* **89** no. 11, (2014) 115022, [arXiv:1404.0022 \[hep-ph\]](#).
- [47] J. Hisano, K. Ishiwata, N. Nagata, and M. Yamanaka, “Direct Detection of Vector Dark Matter,” *Prog. Theor. Phys.* **126** (2011) 435–456, [arXiv:1012.5455 \[hep-ph\]](#).
- [48] J. Hisano, R. Nagai, and N. Nagata, “Effective Theories for Dark Matter Nucleon Scattering,” *JHEP* **05** (2015) 037, [arXiv:1502.02244 \[hep-ph\]](#).